

Review

Online Quality Measurements of Total Suspended Solids for Offshore Reinjection: A Review Study

Dennis Severin Hansen ¹, Mads Valentin Bram ¹, Steven Munk Østergaard Lauridsen ² and Zhenyu Yang ^{1,*}

¹ Department of Energy Technology, Aalborg University, Niels Bohrs Vej 8, 6700 Esbjerg, Denmark; dsh@et.aau.dk (D.S.H.); mvb@et.aau.dk (M.V.B.)

² Total, Britanniavej 10, 6700 Esbjerg, Denmark; steven.lauridsen@total.com

* Correspondence: yang@et.aau.dk; Tel.: +45-4128-7438

Abstract: The importance and awareness of accurate online water quality measurements increase every year in the oil and gas sector, whether it is for reducing oil discharge, preparing produced water for reinjection, or improving operational performance. For online measurement techniques to yield valuable analytical information, an understanding of their outputs must be established. Produced water reinjection has gained increasing attention in the last decade, as it can minimize negative environmental impacts by reducing oil discharge and has the potential to extend the economic life of reservoirs. To increase the amount of produced water that can be reinjected, the water must be maintained at a sufficient quality to prevent unintended formation damage. This review paper thoroughly describes different water quality issues related to suspended solids that can occur in an injection water treatment system and how the issues are often interlinked. A case study of measuring the total suspended solids concentration of seawater sampled from the Danish sector of the North Sea has been carried out to effectively quantify water quality in an injection water treatment facility. Furthermore, numerous on- and in-line techniques have been evaluated as candidates for measuring suspended solids. The last part of the paper discusses considerations regarding future microscopy analyzers based on five promising online microscopy technologies.

Keywords: offshore oil and gas industry; water quality; total suspended solids; online monitoring; injection water treatment; environment



Citation: Hansen, D.S.; Bram, M.V.; Lauridsen, S.M.Ø.; Yang, Z. Online Quality Measurements of Total Suspended Solids for Offshore Reinjection: A Review Study. *Energies* **2021**, *14*, 967. <https://doi.org/10.3390/en14040967>

Received: 17 December 2020

Accepted: 4 February 2021

Published: 12 February 2021

Publisher's Note: MDPI stays neutral with regard to jurisdictional claims in published maps and institutional affiliations.



Copyright: © 2021 by the authors. Licensee MDPI, Basel, Switzerland. This article is an open access article distributed under the terms and conditions of the Creative Commons Attribution (CC BY) license (<https://creativecommons.org/licenses/by/4.0/>).

1. Introduction

Although energy consumption in developed countries is approaching a plateau and entering a new era of climate changes, oil production is still expected to increase during the next 30 years globally, according to Energy Information Administration (EIA) [1]. Figure 1 shows the EIA's projection if no radical changes occurs in energy extraction from 2019 to 2050 while accounting for the expected rising of the world's population. The percentage of total energy production originating from crude oil production is projected to be reduced by 5.5 p.p. from 2019 to 2050. However, crude oil production is still estimated to have an average annual increase of 0.6% from 2019 to 2050, even though European countries who are members of the Organisation for Economic Cooperation and Development (OECD) are estimated to have an average reduction of 4.0% annually from 2019 to 2050.

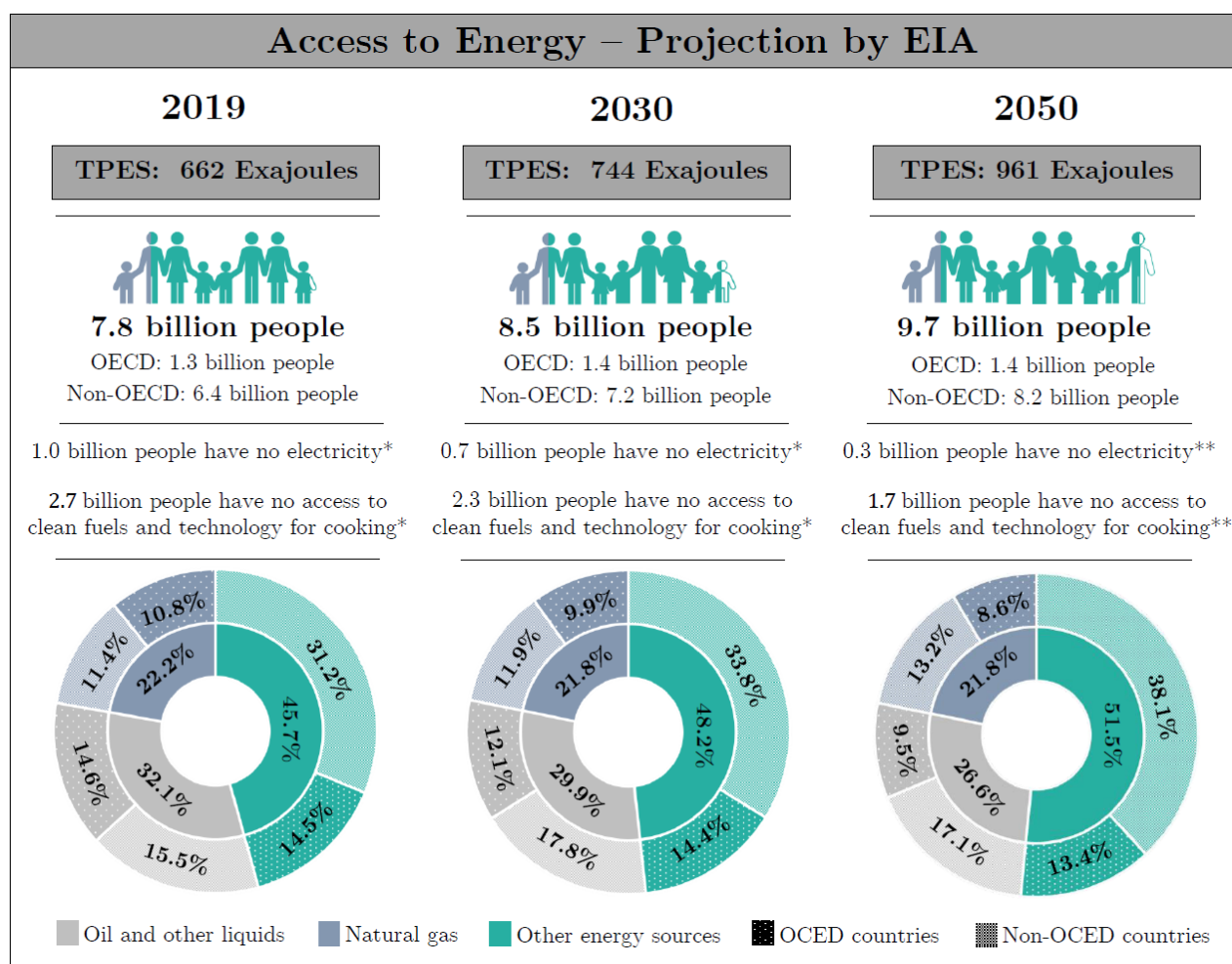


Figure 1. * Based on estimated data from International Energy Agency (IEA) [2]. ** Assuming a continuing gain of 3.34% and 1.40% annually for access to electricity and clean-cooking, respectively, based on the projected data from 2016 to 2030 by IEA [2]. Presented data show the 2050 projection by EIA [3]. The total primary energy supply (TPES) refers to the total amount of primary energy from production and imports subtracting exported energy. Totals may not equal the sum of components as a result of independent rounding. Oil and other liquids include all types of crude oil, natural gas plant liquids, biofuels, etc. [1]. With crude oil being the far biggest source predicted to account for ~82% of the production annually from 2019 to 2050, where biofuels are predicted to account for ~2%. Other energy sources cover coal, nuclear, and renewables, where renewables have the far biggest increase with an average gain of 3.1% in the world and are estimated to surpass energy consumption by oil and other liquids in 2047. Renewables accounted for ~16% in 2019 and are estimated to account for ~28% in 2050 of the world's energy consumption.

The presented results in Figure 1 indicate that the oil and gas industry will have a significant impact on the world's energy consumption in the years to come [3,4]. Therefore, oil and gas recovery strongly incentivizes continual investment in the most innovative solutions by improving energy efficiency and researching new technologies to minimize emissions of greenhouse gas (GHG) [5]. As 70% of the world's oil production originates from brownfields, the by-product of water steadily rises over time, which increases the importance of accurate online measurement of water quality. Online monitoring is generally defined as sampling, analysis, data processing, and reporting of the desired parameters in the process without human supervision [6]. Online monitoring measures more frequently and consistently than manual sampling, allowing automatic supervision of the process' quality or allowing them to be integrated into control operation. Furthermore, online monitoring benefits from executing measurements at inaccessible locations where manual sampling may not be an option.

To comply with future discharge legislation with an increasing water cut, and to gain more sustainable production, produced water reinjection (PWRI) has gained attention [7–10]. PWRI has the potential to extend the reservoirs' economic life, comply with national and local regulations, and minimize negative environmental impacts. To increase the amount of PWRI, the quality of the injected seawater and produced water (PW) must be high and consistent. Effective management of PW and injection water (IW) involves appropriate treatment, discharge, and monitoring. Accurate water analysis is vital to gain an understanding of the dispersed matters of the PW and IW to identify changes in the process. Seen from an economic perspective, accurate information of the amount of oil and particles, their sizes, and classification of particles in the IW can be used for decision support, reporting, and advanced control to achieve better operation in the treatment process [7]. It could also be beneficial to measure other online water quality parameters, such as oxygen concentration and acid concentrations, but this is not the focus of this review study. This paper aims to examine the challenges associated with inadequate IW quality and what effect different water characteristics related to suspended solids can have on a reservoir in the Danish sector of the North Sea. Furthermore, the importance of accurate measurement of total suspended solids (TSS) is analyzed. This analysis is the basis for selecting the most useful online TSS monitor. Even though the different methods and designs of TSS monitors reviewed in this paper are related to offshore IW facilities, most of them are applicable to other domains, such as waterworks and biofuel facilities.

The review study is organized as follows: Section 2 provides an introduction to the main challenges related to waterflooding. Section 3 extensively describes different IW quality characteristics that can affect the TSS concentration and how some characteristics are interlinked. Section 4 presents a case study of measuring the TSS concentration in a benchmarked injection water treatment (IWT) system located in the Danish sector of the North Sea and evaluates the facilities' ability to preserve the TSS concentration after the filtration system downstream. Section 5 addresses the complexity of selecting a suitable method and type for online measurement of TSS in an offshore IWT system. Last, Section 6 provides concluding remarks.

2. Waterflooding

An oilfield is a natural hydrocarbon accumulation in pores of an underground porous media [11]. An oilfield may contain several separated reservoirs linked together, covering a large area. The phenomenon, which leads to the creation of an oilfield, is created by layers of sedimentary materials that are trapped under the weight of overlying layers, resulting in increased temperature and pressure, which induces various chemical reactions, transforming the organic materials into oil over millions of years [11]. These processes finally result in water, gas, and oil being trapped in the reservoir. The reservoir pressure, which commonly exceeds the hydrostatic pressure, transports the reservoir fluids by pipes to the surface. The recovery factor (the recoverable amount of hydrocarbon initially in place) mainly depends on the oil's viscosity, the permeability of the reservoir, the porosity of the reservoir rocks, and the reservoir drive [12]. The amount of oil produced by the reservoir drive is known as primary oil recovery. To increase the oil recovery, an injection fluid can be injected to maintain the pressure and to sweep the reservoir. Waterflooding is defined as secondary oil recovery. However, this still leaves about $\frac{2}{3}$ of oil in place (OIP) [11]. In 1976, the tertiary recovery process was deployed called enhanced oil recovery (EOR) defined as:

"The additional recovery of oil from a petroleum reservoir over that which can be economically recovered by conventional primary and secondary methods" [13].

The main oil recovery stages are as follows

- Primary oil recovery: ~10–15% of OIP
- Secondary oil recovery: ~15–33% of OIP
- Tertiary oil recovery (EOR): ~45% of OIP [11,14]

The optimization involved is not undertaken to increase the oil recovery percentage, but rather to increase the recovery to cost ratio, as when the recovered oil has less value than operational cost, the operation is no longer profitable [13]. This should not be confused with enhanced recovery, which is considered to be a broader definition [11,14]. In fact, any method used to recover more oil from the reservoir than obtained by primary recovery is considered enhanced recovery [13]. However, EOR methods are often referred to as tertiary oil recovery as it is the practical best way to evaluate the incremental amount of oil.

Today, 1% of the total oil discovered is roughly equal to $1/2$ year of the world's energy consumption based on BP's statistical review from 2017 [15]. The 1% of total oil discovered is based on proved reserves. Thus, there is likely more oil left in the reservoirs, which could be economically profitable to extract in the future if: industry practices are improved, new technologies are developed, or the oil price increases. The trend of increasing proved reserves is also supported in BP's statistical review from 2017, as the proven reserves have increased by 48.6% since 1996 [15].

One way of increasing the recovery cost ratio is by focusing on the IW, which has been known for several decades to play a massive role in improving the recovery process [16–22]. Back in 1880, the first waterflooding was executed at Oil Creek, PA (USA), but faced a lot of new and unforeseen issues at that time [17]. Due to the amount of new and unforeseen issues, the expended amount of capital usually ended in unproductive efforts to profitable extract enough oil, and the waterflooding method was postponed. One of the main issues Carll observed was the effect of well short-circuiting, due to IW traveling fastest along the path of least resistance. Therefore, the injection and production wells are carefully placed according to local conditions.

Figure 2 shows a cross section of distributed water injection in a large field. As injection rates are proportional to oil production, it is highly essential to maintain reservoir pressure by controlling the injecting rate [23,24]. First, in the late 1930s, the oil and gas industry rediscovered waterflooding as a potential method in the profitable restoration of old abandoned areas in Bradford and Allegheny fields in the northern part of Pennsylvania and the southern part of New York State [18]. The interests in IW projects steadily increased until the late 1940s—early 1950s—where the progress was immensely accelerated, leading to the expertise of the IWT processes that exist today [16,19–22]. Already in the early years of waterflooding installations in the 1940s, they observed that the quality of the IW profoundly affects the recovery process [19,20].

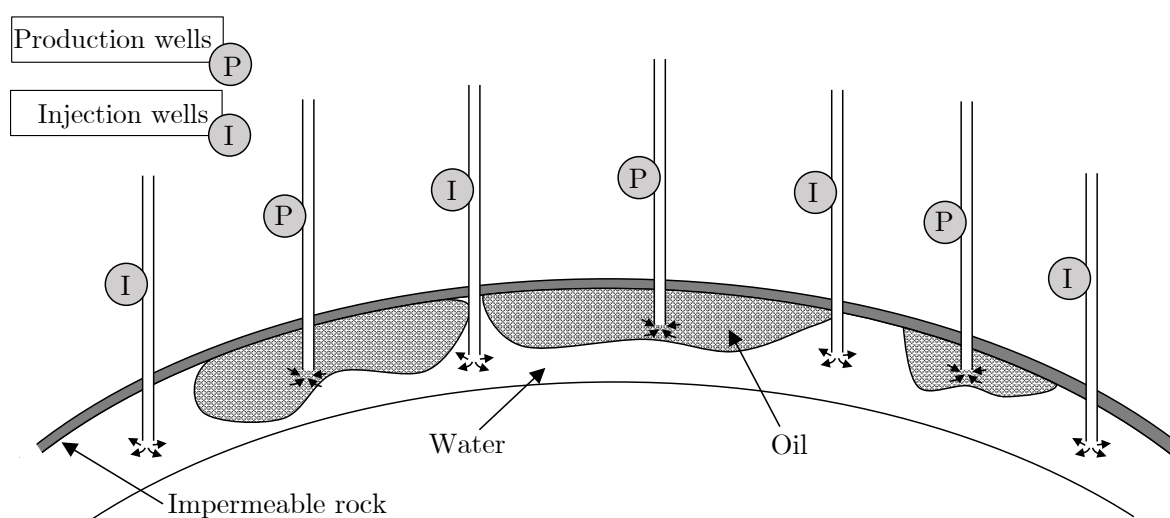


Figure 2. Cross section of a typical large oilfield with distribution of water injection.

Water quality is usually discussed in terms of plugging tendency, which further complicates the process [25,26]. Ideally, IW should be non-scaling sterile fluids free of suspended solids and organic matter to protect the process against corrosion, erosion,

and microbiological growth, which may lead to high maintenance costs for IWT equipment and extensive use of harmful chemicals [27]. However, fulfilling these water quality criteria will not be economically profitable, and the question is, therefore: What are the best economical strategies when balancing water quality and formation damage?

IWT often involves several processes, as described in Section 4, such as filtering, additions of chemicals, and deoxygenation to achieve sufficient water quality, all of which affect both capital expenditures (CAPEX) as well as operating expenditures (OPEX). Sufficient water quality provokes economic incentives to reduce water quality to a required minimum. Conversely, inadequate water quality can result in dramatic formation damage [25,28]. OPEX is necessary to be addressed to establish an economic basis of the IW quality. OPEX includes the cost of chemicals, maintenance, human resources, and energy. If changes in the water quality are preferred, it will thus affect the OPEX. The cost of maintaining the desired IW quality must therefore be balanced against the accumulated production income as a result of changes in the oil recovery rate [25,28].

According to different literature around 1980, the seawater in the North Sea generally has a high quality, with a concentration of 0.2–0.8 mg/L suspended solids, retained by a 0.8 µm filter [29,30]. However, without disparaging the work done back then, the knowledge and technology must be assumed to have advanced since then, and newer results indicate that the mean concentration in the North Sea is 2.6(3.5) mg/L [31], where the parentheses indicate the standard deviation throughout 15-month periods covering the seasonal cycle [31]. Other literature indicate the concentration in the North Sea more loosely as offshore <2 mg/L, inshore (>10 mg/L), in shallow intertidal areas (50–100 mg/L, and up to 2000 mg/L) and 20 km offshore ~4 mg/L [32,33]. The different terms of particle scale sizes and their corresponding classification from the cited literature is shown in Table 1. The percentiles in mm-transformation is given by the relation

$$\phi = \text{Log}_2 D, \quad (1)$$

where D is the diameter of the measured sediment unit [34].

As previously described, water quality is usually discussed in terms of TSS and their plugging tendency. Other water quality characteristics can directly or indirectly affect the plugging increment and be part of the TSS concentration [26]. Thus, TSS concentration can consist of several water quality characteristics and mechanisms of formation damage. In terms of TSS, the various water quality characteristics are described in Section 3.

Table 1. Particle size scales and terminology by different litterateurs [35–37].

mm	ϕ	Udden (1898) [35]	Wentworth (1922) [36]	Blott and Pye (2012) [37]
2048	−11		Boulder gravel	Megaclasts
1024	−10			Very large boulder
512	−9			Large boulder
256	−8			Medium boulder
128	−7		Cobble gravel	Small boulder
64	−6			Very small boulder
32	−5		Pebble gravel	Very coarse gravel
16	−4			Coarse gravel
8	−3			Medium gravel
4	−2	Coarse gravel		Fine gravel
2	−1	Gravel	Granule gravel	Very fine gravel
1	0	Fine gravel	Very coarse sand	Very coarse sand
1/2	1	Coarse sand	Coarse sand	Coarse sand
1/4	2	Medium sand	Medium sand	Medium sand
1/8	3	Fine sand	Fine sand	Fine sand
1/16	4	Very fine sand	Very fine sand	Very fine sand
1/32	5	Coarse dust	Silt	Very coarse silt
1/64	6	Medium dust		Coarse silt
1/128	7	Fine dust		Medium silt
1/256	8	Very fine dust		Fine silt
1/512	9	(Clay)	Clay	Very fine silt
1/1024	10			Very coarse clay
1/2048	11			Coarse clay
1/4096	12			Medium clay
1/8192	13			Fine clay
				Very fine clay

Several studies have previously highlighted water quality as the key to maintain a consistent waterflooding and how the water quality can affect the injection rate of an IWT facility [21,25,26,38–43]. Most of the studies focus on operation design solutions to keep high and consistent water quality. The importance of monitoring the TSS concentration in the process is highlighted in a few studies, e.g., Patton [26], Bennion et al. [41], Donham [43], and Ogden [42]. However, none of them address the complexity of analyzing particle morphologies continuously and the considerations when selecting online monitors to increase the water quality.

3. Injection Water Characteristics and Formation Damage Mechanisms

Two factors determine the sufficient quantities and acceptable quality of the IW: the geological formation and geographical location of the reservoir [44]. A reservoir with high porosity and high permeability tends to sustain its injection rate longer [45].

Porosity is a measure of the pore volume between sediment grains in the reservoir that can contain fluid or gases, and permeability is a measure of the flowability through the reservoir rocks. Thus, the total volume of oil, water, and gas that are present in a reservoir depends on the porosity. The porosity value is higher when the sediment is well sorted and has a well-packed structure. Porosity is the ratio of the pore volume, V_p , and the total volume, V_T , of the reservoir sediment/rock.

$$\Phi = \frac{V_p}{V_T} \cdot 100 \quad (2)$$

The permeability is also higher in well-sorted sediment but depends highly on the grain size due to the fluid flows easier in large pores than in small ones. Permeability, therefore, indicates how easy it is to produce oil or gas. It is mathematically expressed with Darcy's law:

$$k = -\frac{q\mu\Delta L}{A\Delta p}, \quad (3)$$

where k is the permeability, q is the flow rate, μ is the fluid viscosity, A is the cross-sectional area of the measured volume, Δp is the pressure drop, and ΔL is the length of the measured volume. Permeability is often measured in millidarcy (mD), and the permeability of oil and gas reservoirs ranges from 0.1 to 3000 mD [46]. The Danish sector of the North Sea is estimated to have a relatively high porosity of 34–40%, but a low permeability 0.1–10 mD, as the Danish reservoirs often consist of chalk [47,48]. Chalk reservoirs are mainly composed of single-crystal lathes of calcite produced by the disaggregation of coccoliths [49]. These pore throat sizes range from 0.1 to 1 μm [49,50]. The presence of TSS in the IW can result in rapid injectivity reduction of the injection well, especially due to pore throat sizes in chalk reservoirs. Predicting the well impairment from TSS has been investigated in several studies [38,51,52].

For determining the different influences of the IW quality characteristics related to TSS, a block diagram is illustrated in Figure 3, followed by a description for each of the IW's characteristics and their formation damage mechanisms. Figure 3 only presents the main root cause's mechanisms of formation damage by the different water quality characteristics, and different mechanisms may interact.

To ensure the quality of the IW fulfills certain criteria for the specific formation, operators must have confidence in the data generated from the measurement equipment. Action mislead by inaccurate measurements can cause more harm than not taking any action at all [28,42,53]. The main IW quality characteristics are described in the following subsections: Oil Content (Section 3.1), Total Suspended Solids (Section 3.2), Total Dissolved Solids (Section 3.3), Dissolved Gases (Section 3.4), and Bacterial Growth (Section 3.5).

3.1. Oil Content

Historically, mostly seawater has been used as IW, but due to the increasing environmental awareness, the discharge policy may require PWRI by means of further reducing the discharge of crude oil. According to the literature, zero discharge policy has become the norm in the industry [8,9,54]. However, in far most cases, there is not enough PW to satisfy injection demands. Therefore, the solution is often a mixture of PW and seawater [55]. In 2019, Gorm-field was the only field from which PW is expected to be reinjected in the next five years, as there are technical reservoir challenges in PWRI at other fields in the Danish sector of the North Sea [56]. According to the Danish Environmental Agency [56], 4.8 million m^3 was projected to be reinjected; thus, only 14.5% of the total 33.0 million m^3 IW was expected to consist of PW in 2019.

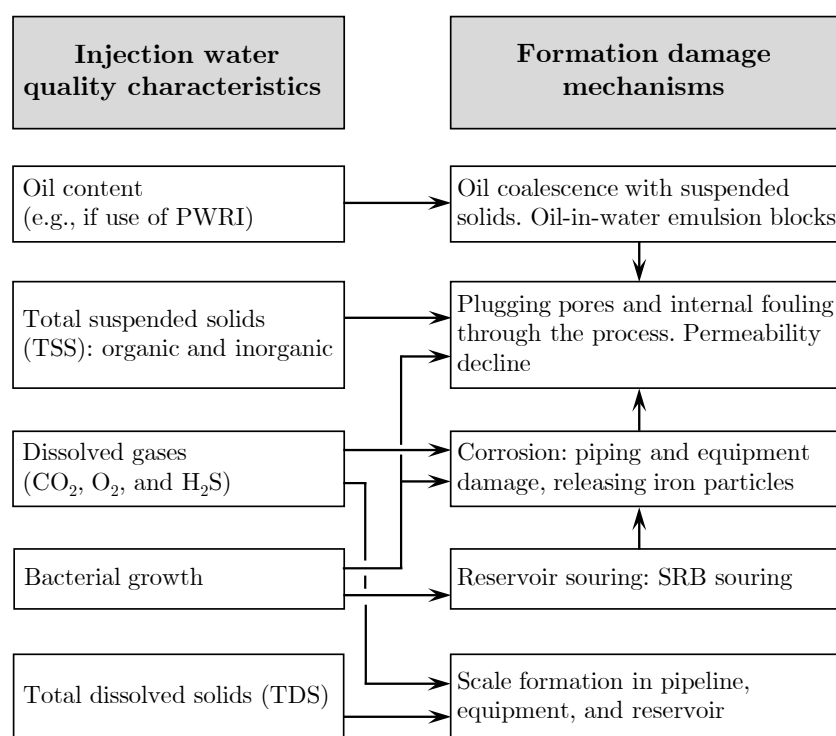


Figure 3. Main potential water quality characteristics and mechanisms of formation damage.

As the water cut in the Danish part of the North Sea steadily increases annually and has reached 80% in 2015, as shown in Figure 4, a high amount of energy is required to handle these large volumes of PW. For some of the matured fields, the water cut even exceeds 90% [45,57,58].

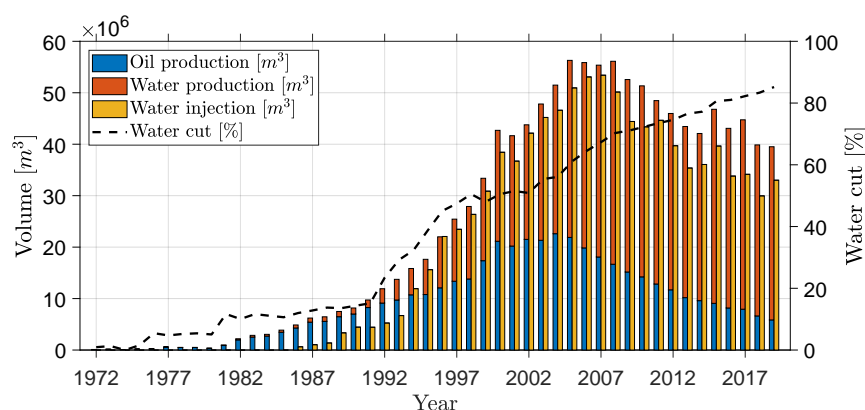


Figure 4. The bar chart shows the yearly oil and water production, water injection, and the water cut. The production data are based on annual reports from the Danish part of the North Sea, published by Danish Energy Agency 1972–2019 [59].

In the North Sea, the discharge legislation declares that the PW must contain less than 30 parts per million (ppm) of oil. Furthermore, the Danish Environmental Protection Agency declares that the total amount of discharged oil in the Danish sector of the North Sea must be less than 222 tonnes per year in 2019/2020 [54–56,60]. As an increasing amount of water is produced, the limit of the total discharged oil becomes more significant, especially as some oil producers in the Danish sector of the North Sea reached 96% of the total amount of discharged oil in 2015 [54,61]. In 2014, the Oslo and Paris Convention (OSPAR) commission reported that 16 installations failed to meet the 30 ppm discharged legislation, where each of the installations exceeded an annual average concentration of dispersed oil discharge [62]. Several of them reported that the reason for not complying

with the discharge legislation was due to PWRI failure. Based on these reports, they might not consider the concentration of oil when reinjecting PW. The crude oil can reduce the injectivity in several ways, e.g., emulsion blocks and flocculation, where the oil droplets work as an agglomeration whereby particles form larger-sized clusters that can block pores in the porous media. Emulsions are formed when a mixture of oil and water are exposed to intense mixing [63]. This intense mixing creates high shear forces and leads to stable OiW emulsions.

Unfortunately, mixing seawater and PW can result in several other complications than just the presence of crude oil. Additionally, PW contains other organic nutrients and purification chemicals from the upstream production process, which may result in ideal conditions for bacterial growth, an increment of scales, and corrosion in the IWT process [8]. Another considerable issue of crude oil content is the deposition of suspended organic solids, such as asphaltenes, which have been shown in the literature to decrease the oil production to such a degree that few have prematurely stopped producing in Saudi Arabia [63]. Bacterial growth, scales, corrosion, and asphaltenes will be described in the Sections 3.2–3.5.

3.2. Total Suspended Solids

To determine whether or not a particle is defined as part of TSS or total dissolved solids (TDS), it is essential to address the standard definition for the examination of water and wastewater determined by the American Public Health Association, American Water Works Association, and Water Environment Federation [64]. The overall definition of TSS and TDS is called total solids, which is defined as follows:

Total solids—The material left in a sample vessel after evaporation and subsequent oven drying at a defined temperature. Total solids include both total suspended and total dissolved solids, which are physically separated via filtration whether a solids particle is filtered into the “suspended” or “dissolved” portion principally depends on a filter’s thickness, area, pore size, porosity, and type of holder, as well as the physical nature, particle size, and amount of solids being filtered [64].

Thus, TSS and TDS are defined as follows:

TSS—The portion of total solids in an aqueous sample retained on the filter. Note: Some clays and colloids will pass through a 2 μm filter [64].

TDS—The portion of total solids in a water sample that passes through a filter with a nominal pore size of 2.0 μm under specified condition [64].

If only considering the “Total solids” phrase, particles retained by the selected filter are considered as TSS. Thus, TSS can consist of any substances present in seawater and PW: inorganic materials, microorganisms, shells, scales, asphaltenes, clays, etc. TDS (TSS that passes the filter) can also represent a wide range of substances and cause different complications further in the treatment process or formation damages.

However, the “TSS” and “TDS” phrases include extra information that the nominal pore size of the filter must be 2 μm ; this concludes that portion of total solids retained by a 2 μm filter is considered as TSS and matters that pass through the filter is considered as TDS. This definition might be confusing and problematic when other papers address TDS as “dissolved”, which usually refers to a solvent that is soluble in a solution, like salt in water or at least TSS above the molecular range [65]. Table 2 provides an overview of different literature’s definition of TDS and TSS. The rest of this work only defines TDS as materials that are soluble in water and TSS as any suspended solids that can be captured by a filter.

Table 2. Different definitions of TSS and TDS.

Definitions Used in Different Studies	Source
TDS defined as materials that are soluble in water	[42,55,65]
TDS defined as materials that passes through a 2 μm filter	[66,67]
TDS is indirectly defined as materials that are soluble in water	[45,68,69]
TDS is indirectly defined as materials that passes through a 2 μm filter	[21,25,43,70]
Too uncertain to tell	[39–41,44]

TSS is considered a significant issue that reduces water quality and injectivity [41]. TSS' progression through the porous media is a complicated process determined by several factors such as shapes, sizes, the concentration of TSS, the chemical composition of the carrying fluid, the mobilization in the reservoir, and the porosity and pore space in the reservoir. A combination of all influences acting upon the TSS affects the outcome of the TSS' progression through the porous media, whether they pass through the porous media or becomes a part of the plugging mechanisms [45]. The flow velocity of the carrying fluid also affects the travel distance of particles inside the porous media. Larger particles tends to settle faster than smaller ones, and particles with higher density difference than the carrying phase similarly tends to settle faster [45]. Plugging mechanisms distinguish between internal or external cake formation. External cake formation potentially consists of larger particles sealing the pore throat either by itself or by bridging, and internal cake formation happens when small particles invade the pore throats and settle within the pore bodies, either by bridging or decreasing the pore volume due to adsorption or sedimentation [41,45,71]. The four main different plugging mechanisms are illustrated in Figure 5.

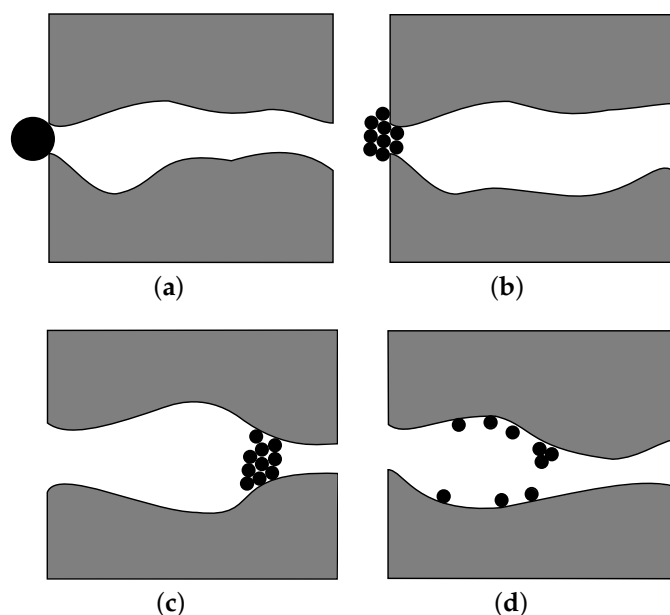


Figure 5. A set of the four main different plugging mechanisms that can occur in the porous media: (a) Illustration of complete external cake formation by single suspended solid. (b) Illustration of external cake formation due to larger suspended solids bridging. (c) Illustration of internal cake formation due to small suspended solids bridging. (d) Illustration of internal cake formation, due to surface deposition.

Ideally, a filter system that can persistently clean water from TSS will massively reduce the possibility of cake formation in the reservoir and bacterial growth, which will further reduce corrosion in the system. However, this will likely not be economically feasible. Therefore, some significant factors influencing the overall cost of selecting the right cost-

effective filtration system must be treated: reservoir medium size distribution, filter pore size distribution, the critical flux of the filters, filtration cost, filtration replacement frequency, maintenance, chemicals, and energy use [72]. The most crucial factor of the filter is to ensure no or minimum clogging of the porous media in the reservoir. Therefore, filters are selected based on the reservoir porosity/size distribution and the desired bridging factor, like Abrams rule [73]. From the literature, filters operating below the critical flux are more economical because of lower energy requirements [71,74]. Filtration below the critical flux is also desirable, as fouling remains irreversible, and the filtration system can be operated in a clean regime. Reducing the filters' pore size reduces critical flux, and the filtration system is forced to perform a cleaning procedure more frequently. Operation above the critical flux causes fouling, which reduces the critical flux over time.

Bridging of particles is a commonly known phenomenon [30,45,75]. Abram proposed, as a rule-of-thumb, that particles larger than $\frac{1}{3}$ of the pore diameter can form an external filter cake due to bridging, and particles smaller than $\frac{1}{7}$ of the pore diameter are passing through without creating any cake formation [45,76]. This has, for several years, been generally acceptable guidance for selecting the right filter for the treatment process. However, several experimental studies have proved that due to porous media's complex nature, a simple norm is inadequate for describing filtration limit [40,41,73,75]. Van Oort et al. [73] suggested adjusting the $\frac{1}{3} - \frac{1}{7}$ rule-of-thumb, based on new investigations, to $\frac{1}{3} - \frac{1}{14}$, which may be more applicable especially at low injection velocities. Newer investigations of TSS have even observed stable bridging of particles in laminar flow with sizes below $\frac{1}{14}$ of the pore size in porous media [41]. A fundamental issue of using the $\frac{1}{3}$ rule-of-thumb for IWT processes arises as Abrams rule only defines that particles should be at least $\frac{1}{3}$ of the pore's size to effectively form bridging and not the opposite [76]. This does not conclude that particles below $\frac{1}{3}$ of the pore size cannot form a stable bridge and creating cake formation, which some newer studies also indicate by concluding that internal cake formation happened for particles below $\frac{1}{14}$ of the porous media pore size distribution.

The selection of optimum filtration criteria would suggest a filtration pore size distribution of $\frac{1}{14}$ of the porous media pore size distribution. This is likely impractical and not economically feasible, especially not in chalk reservoirs due to its small pore sizes.

As TSS represents a wide range of substances, some TSS types may not be readily removed by the filtration, like asphaltenes. Asphaltenes are the heaviest component in crude oil [77]. Under the initial condition of the reservoir, asphaltenes are dissolved in crude oil, but as the reservoir is exposed to changes in temperature and pressure, it may affect the asphaltenes to precipitate from the crude oil [41]. Asphaltenes are highly polar and tend to have an attraction property, as individual micelles attract one another, forming large particle sizes of asphaltenes [41]. Consequently, usual filtration media are often ineffective in removing the asphaltenes, as the individual asphaltene particles break up in order to pass and coalesce on the other side. The coalescence is very time-dependent, making long transportation pipelines a good condition for coalescence to occur after the filtration process. Some systems have recorded particles up to 100 times the sizes of particles expected after the filtration system further down the treatment process [41]. Asphaltenes have the ability to form a viscous coating layer on filter elements in the transportation pipelines and the reservoir. Asphaltenes are also known to stabilize emulsions [63]. As mentioned in Section 3.1, several wells in some fields in the northwestern part of Saudi Arabia have shown an atypical productivity decline. Production was halted even at water cuts as low as 25%, with the presence of asphaltenes as the primary reason [63].

Another suspended particle that has a unique behavior as asphaltenes is clay. Clay swelling has, for a long time, been recognized as a cause of formation damage in reservoirs [40,77–80]. Clay minerals are extremely small platy-shaped particles smaller than 8ϕ as shown in Table 1 [77]. Even though clay-related problems are often mentioned in relation to well operation, such as drilling processes, they also occur in IWT processes [78,79]. Reduction in permeability due to clay swelling occurs as a result of decreases in pore body

or pore throat size as the volume changes of the clay [79,80]. The phenomenon of clay swelling is a negatively charged imbalance in the clay structure, which are stabilized by substitution of a positively charged cation (i.e., Na^+ , K^+ , Ca^{2+} , and Mg^{2+}) into the gap between the individual clay crystals [40]. If an insufficient concentration of these ions is not present around the clay, water can interact with the clay due to its polar nature. This causes the clay to physically swell and can cause severe reductions in the reservoir's permeability as it can expand up to 20 times its original volume [81]. Another phenomenon of clay action is clay deflocculation. Clay deflocculation is caused by the disruption of electrostatic forces, causing the clay to be attracted to each other and act as agglomeration for other particles. Clay swelling have also been reported to cause disengages from the pore walls due to the expansion and consequently transported further down in the pore body until it hits the pore throat area. Thus, they additional acts to bridging or complete pore blocking [40,78].

3.3. Total Dissolved Solids

TDS concentration is a quantification of the cations and anions in the IW. A high concentration of TDS in the IW can cause scales to build up in pipelines and instruments. Scales increase the injection resistance, resulting in a decrease in injectivity over time. In the worst case, it will completely plug the injection trains and equipment. Other consequences could cause equipment failures, emergency shutdowns, increased maintenance costs, and, seen from a production point of view, decreased production efficiency [82]. Scale deposition can occur due to supersaturations of the IW. However, supersaturation does not necessarily produce scales; there must be a presence of nucleation. Scale formation is mainly caused by supersaturated conditions, which occur when higher concentrations of dissolved solids are presented in the IW than their equilibrium concentration [83]. Supersaturation can occur by changes in pressure and temperature conditions or when two incompatible water types are mixed [84]. Changes in pH, carbon dioxide (CO_2), and hydrogen sulfide (H_2S) could also induce scale formation [84]. Seawater can contain a significant concentration of sulfate (SO_4^{2-}) and carbonate (CO_3^{2-}) ions, while formation water contains cation ions of calcium (Ca^{2+}), barium (Ba^{2+}), and strontium (Sr^{2+}) [85]. When these two water types mix, supersaturation can occur, which causes calcium carbonate (CaCO_3), calcium sulfate (CaSO_4), strontium sulfate (SrSO_4), and barium sulfate (BaSO_4) to deposit, as shown in Figure 6 [85]. Other less common scales have also been reported, such as iron oxide (Fe_2O_3), iron sulfide (FeS), and iron carbonate (FeCO_3) [85,86].

Cations:		Dissolved solids:
Sodium (Na^+)	→	Sodium Chloride (NaCl)
Calcium (Ca^{2+})		Calcium Carbonate (CaCO_3)
Iron (Fe^{2+})		Calcium Sulfate (CaSO_4)
Barium (Ba^{2+})		Barium Sulfate (BaSO_4)
Strontium (Sr^{2+})		Strontium Sulfate (SrSO_4)
Anions:		
Chloride (Cl^-)	→	Iron Carbonate (FeCO_3)
Carbonate (CO_3^{2-})		Iron Sulfide (FeS)
Sulfate (SO_4^{2-})		Iron Oxide (Fe_2O_3)
Sulfide (S^{2-})		
Oxide (O^{2-})		

Figure 6. Chemical formula and formation of mineral scales.

3.4. Dissolved Gases

Seawater contains different dissolved gases, where the troposphere is the primary source of gases to seawater. The gases enter or leave the ocean by exchange across the interface between seawater and troposphere [87]. Dissolved gases in the injection process can result in several complications. The two main reasons for removing/reducing dissolved gases are corrosion and the growth of aerobic organisms. There will only be focused on corrosion influenced by dissolved gases in this subsection. The presence of oxygen (O_2) in the IW and its effects on aerobic organisms will be addressed in the Section 3.5.

The three main dissolved gases that cause corrosion in the oilfield industry are O_2 , CO_2 , and H_2S [88–90]. When CO_2 and H_2S are dissolved in the water, they form acids. As the concentration of CO_2 and H_2S increases, the pH of the IW will continue to decrease, creating a corrosive environment [42,91]. In the oil and gas industry, CO_2 -corrosion is often referred to as sweet-corrosion and H_2S -corrosion to as sour-corrosion, where the presence of O_2 can be several times more corrosive than CO_2 and H_2S [92,93]. A comparison between different concentrations of O_2 , CO_2 , and H_2S in water shows that O_2 is 80 times and 400 times more corrosive than CO_2 and H_2S , respectively [88,93]. Corrosion detected in the oil and gas industry involves several mechanisms divided into three different corrosion effects: electrochemical corrosion, chemical corrosion, and physical corrosion, where each corrosion effect covers several types of corrosion [94,95]. Figure 7 lists some of the corrosion types that can exist. However, this study will not cover each corrosion type but only draw attention to the existence of different corrosion effects mentioned in different papers [88,91,92,96].

Electrochemical corrosion	Chemical corrosion	Mechanical effects
Galvanic corrosion	Sour corrosion	Cavitation corrosion
Crevice corrosion	Sweet corrosion	Erosion corrosion
Stray current corrosion	Oxygen corrosion	Environmental induced cracking
Pitting corrosion	Concentrated brines	Corrosion fatigue
Intergranular corrosion	Biological effects	Fretting corrosion
Uniform corrosion	Strong acids	

Figure 7. Categorized corrosion effects.

Corrosion has a huge economic impact on the industry; its influences are estimated to cost 1.3\$ billion annually in the oil and gas industry in the US alone [88–90,92]. Of the total annual corrosion cost, 43% originates from surface pipeline and facility costs, 34% from downhole tubing expenses, and 23% from other corrosion-related costs [89]. Corrosion is a natural mechanism, as metals tend to return to their natural state by reacting with oxidizing agents present [97]. For corrosion to occur, it requires four elements: anode, cathode, electrolyte, and a metallic/electronic path [95,98]. All metals will eventually dissolve or corrode to some degree; the process is illustrated in Figure 8 [88]. A typical corrosion process occurs as two dissimilar metals are present in an electrolyte. The anode is the metal that forms the negative pole, and the metal that forms a positive pole is the cathode. The conducting solution (IW) is the electrolyte, and the return path for electronic current flow is through the pipeline metal between the anode and cathode, as shown in Figure 8 [98].

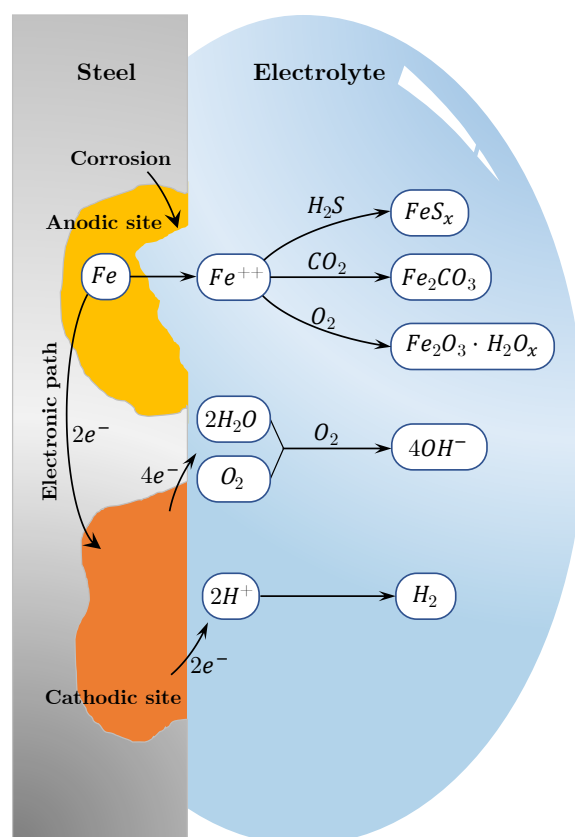


Figure 8. Corrosion on a steel surface due to reaction with the reaction fluid, present of O_2 , CO_2 , or H_2S . Inspiration from the work in [88].

As the anodic site releases electrons to the cathode site, Fe^{2+} reacts either with O_2 , CO_2 , or H_2S , which forms the corrosion products: iron sulfide (FeS_x), iron carbonate ($FeCO_3$), or iron oxide ($FeO_3 \cdot H_2O_x$), that are often referred to as rust or corrosion deposits [88,92,93]. However, if no dissolved gases are present to react with Fe^{2+} , the tendency to dissolve will heavily be diminished. The O_2 level required to prevent corrosion must be lower than 0.025 ppm, as O_2 concentrations above accelerates corrosion, according to different studies [30,99,100].

Wall thickness reduction is the most considerable risk for pipeline failures [101]. According to data in the period of 1994–1999, 25% of all accidents were due to corrosion in transportation pipelines [102]. When corrosion products are not deposited on the pipelines' surface, very high corrosion rates can reduce the pipeline wall thickness several millimeters per year [91]. Figure 9 shows three gas concentrations as a function of corrosion rate on carbon steel per year. It clearly shows that over time, with no maintenance, the wall thickness is reduced to such a degree by corrosion that the pipeline will crack in the corroded area causing leaks or damage to the entire pipeline system [103,104].

The deposit formation of corrosion acts as TSS; even if the IW is free from TSS after filtration, the TSS concentration can increase through the process [99]. Changes in the internal surface roughness can be another side effect of corrosion. The pipelines' internal surface roughness is a pipeline system design criteria, and changes of surface roughness can have economic expenses. The surface roughness impacts the flow regime in a pipeline due to friction and thereby creating undesired energy losses [105].

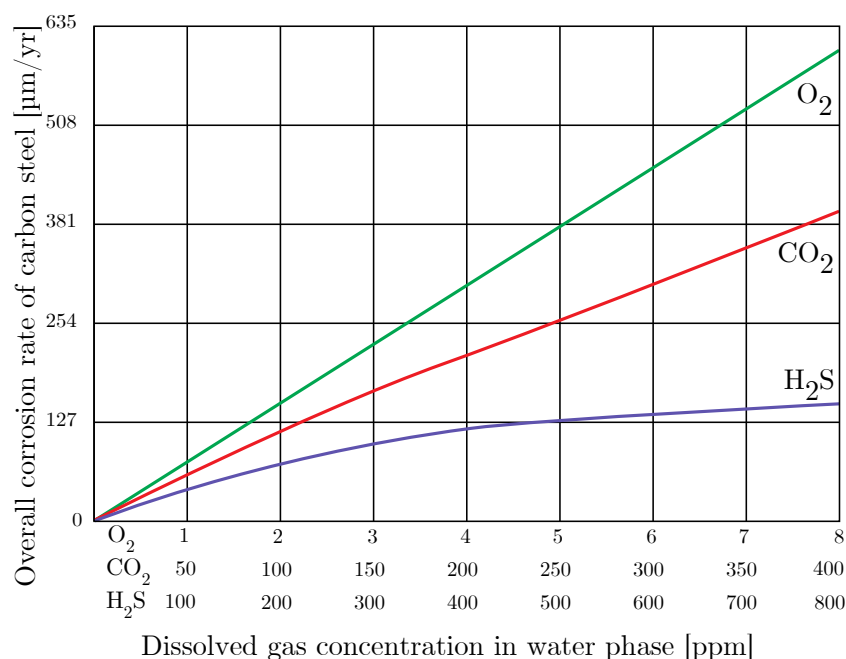


Figure 9. Comparison of corrosion rates exposed to different concentrations of O₂, CO₂, and H₂S dissolved in water [88]. Schlumberger. All rights reserved.

3.5. Bacterial Growth

Although the significant effects of microorganism activities in the oil and gas industry were recognized a long time ago, little is known about the effects in the reservoir when continuously introducing microorganisms via waterflooding [106–108]. Microorganisms can cause or contribute to plugging pores and internal fouling throughout the process and accelerate corrosion of pipelines and equipment. Microorganisms are a highly diverse group of microscopic single-celled organisms and viruses. However, viruses are not considered as an issue in the oil and gas industry as they are extremely small, mostly ranging from 0.02 to 0.4 μm, and viruses are not considered as living organisms as, unlike bacteria, viruses cannot reproduce on their own [109,110]. Microorganisms, other than viruses, fall into two classifications: the prokaryotes and eukaryotes. Prokaryotic microorganisms include bacteria and archaea, and eukaryotic microorganisms include algae and fungi [111]. It is estimated that there exist $(4 - 6) \cdot 10^{30}$ prokaryotic microorganism types worldwide and $1.2 \cdot 10^{29}$ occur in the ocean [112,113].

Classification of bacteria is essential for identifying which bacteria are present. Figure 10 shows how the classification often is carried out [114]. Classifying bacteria is often started on the morphological elements of the organisms, such as shapes, sizes, and colonies, as shown in Figure 11 [115].

Together with the Gram stain method, Gram-negative and Gram-positive, the microorganisms can be classified into different groups based on the morphological elements. Gram-positive cell walls have a thick murein layer and a cell membrane, whereas Gram-negative cell walls have an outer membrane and a thinner murein layer. The Gram stain method then stains the Gram-positive microorganisms' violet and the Gram-negative microorganisms pink due to their murein layer. Other steps for classifying the microorganisms are based on their atmospheric growth, biochemical properties, antigenic properties, and growth characteristics, such as temperatures and pH [115]. Most recently, next-generation sequencing (NGS) is used to understand the evolution of bacteria and their connections to other organisms [115].

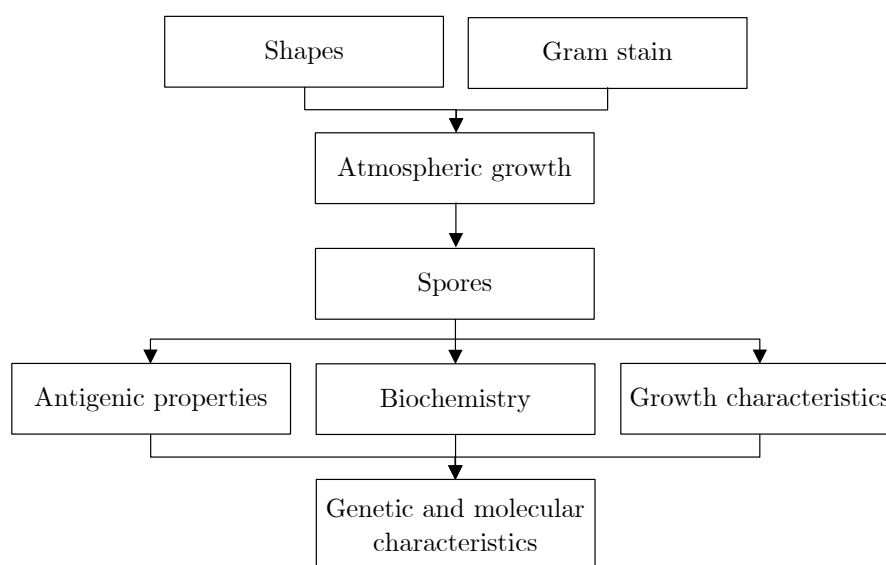


Figure 10. Bacterial taxonomy: classification and identification methods [115].

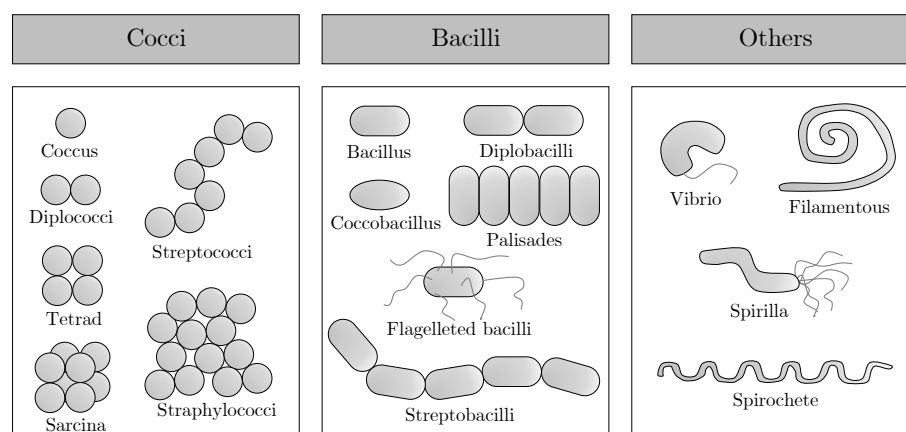


Figure 11. Bacteria come in a variety of shapes, the most common being varieties of cocci and bacilli. Cocci have a spherical, ovoid, or generally round shape and can occur singularly and as groups. They have the ability to stick together and form a pair (diplococci), in long chains (streptococci), and irregularly shaped clusters (staphylococci). Rod-shaped bacteria are called bacilli and occur as single rods or in long chains. Spiral- or helical-shaped bacteria are called spirilla, and vibrio has a curved-rod shape (comma shape) [116].

Microorganisms require water, nutrients, and electron acceptors for growing, where growth involves both an increase in the size and population [117]. Different bacteria have evolved to grow and survive in widely differing habitats. Whereas nearly all eukaryotic organisms require O_2 to multiply, many species of bacteria can grow under anaerobic conditions [67]. Bacteria are frequently classified in terms of the following growth characteristics.

- Obligate aerobic bacteria require O_2 to multiply.
- Obligate anaerobic bacteria multiply in the absence of O_2 .
- Facultative anaerobic bacteria can multiply in both the presence and absence of O_2 due to its metabolism.
- Microaerophilic bacteria need the presence of O_2 . Though, at high concentrations of O_2 , they are poisoned.
- Aerotolerant microorganisms multiply in the absence of O_2 . Though they are not poisoned by O_2 [117].

Even though obligate anaerobic microorganism cannot grow in an O₂ environment, an excellent place to live for an anaerobic organism is below an active colony of aerobic organisms as these consume the O₂ and create anaerobic zones, which serve as habitats for the anaerobic microorganisms [118]. Thus, obligate anaerobe microorganisms, such as sulfate-reducing bacteria (SRB), can survive and multiply below aerobic habitats as they are protected by aerobic organisms [118].

Temperature greatly influences the growth and survival of microorganisms. There is a minimum temperature below which growth no longer occurs for each specific type of microorganism, an optimum temperature range at which the growth is most rapid, and a maximum temperature above which growth is not possible. Other influences on the growth of microorganisms are the pH and salinity concentration.

Most types of marine bacteria can grow in temperature ranging from 0 to 40 °C, although some types can survive even above 100 °C [40,119]. Even when deep formations surpass temperatures for bacterial growth, in many cases, around the injection wells, a tempered formation can occur due to the long-term water injection. This may result in severe bacterial growth problems down in the reservoir, especially if a biological activity was not considered as an issue [40].

When microorganisms play a role in IWT processes, they are often referred to as microbially influenced corrosion (MIC) and biofouling. MIC has become an acknowledged phenomenon in the oil and gas industry the last decades, starting back in the early 1990s, even though there has been an awareness of maintaining a degree of microbial cleanliness in the IWT processes long before that [106,120,121]. MIC is estimated to account for 20–30% of all corrosion-related costs in the oil and gas industry, and other studies even report it to account for 50% of the total cost of corrosion [104,106,121,122]. Microorganisms do not produce unique types of corrosion; instead, they accelerate some of the corrosion types mentioned in Section 3.4, like pitting and stress corrosion [121]. One of the most recognizable presence of MIC is related to reservoir souring, which defines the increasing H₂S level as mentioned in Section 3.4, especially in a reservoir that initially did not consist of any H₂S [123]. The increasing level of H₂S is often a result of SRB growth in the process.

Biofouling activities in IWT processes can cause materials deterioration and mechanical blockages of fluid transport systems that consequently increase energy consumption [124]. Often, biofouling activities in IWT processes are referred to in the filtration system. Biofouling has been known as a contributing factor to more than 45% of all filter fouling and has been reported as a significant problem in membrane filtration by reducing flux rates, increasing the amount of reject water, decreasing permeate quality, and reducing the lifetime of membranes [125].

For both biofouling and MIC, biofilm formation is the root cause. A biofilm is an agglomeration assemblage of microorganisms that are enclosed in an extracellular polymeric substance (EPS) matrix of mainly polysaccharide material [126]. EPS is often referred to as “slime” due to its consistency [118,126].

Figure 12 indicates four biofilm stages, where each stage represents different development stages. Biofilm provides a local ecosystem in which the organisms can multiply [118,127]. The biofilm often consist of different microorganism types; even microorganisms that are unable to attach to the surface on their own can still attach themselves to the EPS or directly to the earlier development of the colony [128,129]. The multiplication of bacteria inside the biofilm still has its own optimum growth parameters [121]. During the biofilm formation, the outer layers become aerobic and the inner layers become anaerobic [130].

One of the biggest challenges with the presence of biofilms in a system is their tolerance to biocidal agents (e.g., chlorine). Studies have proven that biofilms can tolerate up to 1000 times higher concentrations of biocidal agents than planktonic cells [126,130,131]. Biofilms have even been observed in the disinfection pipelines of biocides [118]. Biofilm is resistant to other harsh conditions such as extreme temperatures, pH, high turbulence, and exposure to ultraviolet (UV) light [118]. Another critical characteristic of biofilm is the ability to change the *in-situ* ecosystem from its surrounding; it can change the pH

more than three units locally [118,132]. Thus, water samples do not reflect changes in pH value; the pH value can differ significantly in the biofilm from the water phase, where the corrosion process is often taking place.

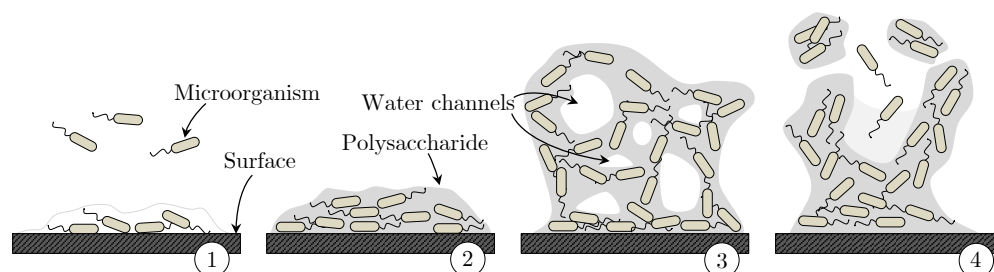


Figure 12. (1) Stage indicates free-floating biofilm-producing bacteria that adhere to the surface of pipelines, filters, equipments, etc. (2) Stage form colonization inside EPS, and the attachment becomes irreversible. (3) Stage biofilm is formed and the *in-situ* ecosystem is growing by creating water channels allowing the water to keep the biofilm hydrated and nourished [127]. (4) Stage reaches critical environmental factors such as the mass or nourishment of the biofilm, that either disperses or colonizes on surfaces further down.

Biocides are traditionally added to IWT processes to remove biofilm, controlling the MIC, and prevent H_2S production, but the misapplication of biocides can lead to significant issues, including resistance or lack of susceptibility to biocide treatment [133,134]. The primary objective of biocides is to limit the multiplication of numerous microorganisms, but according to Little et al. [134] neither oxidizing (e.g., chlorine) nor non-oxidizing (e.g., glutaraldehyde) biocides can penetrate biofilms. The effectiveness of biocidal agents is highly dependent on the types of microorganism present [135]. One of the main issues with MIC is the number of different species; there is no single biocide that encounters all conditions. Therefore, biocides are chosen based on several factors: cost, environmental toxicity, ease of disposal, effectiveness at targeting the unwanted activities, and effectiveness at low concentrations [135,136]. However, operators' biggest concerns are related to the effectiveness of long-term chemical treatments, as it is difficult to predict and measure the effectiveness accurately [136].

As an alternative to biocide treatment, the injection of nitrate has been demonstrated to reduce the amount of SRB and their activity, known as bio-competitive exclusion [134,137–139]. The injection of nitrate can induce a shift in the dominant population from SRB to nitrate-reducing bacteria (NRB) [134]. The primary purpose for nitrate addition is to create competition for nutrients, as when NRB and SRB are competing for the same nutrients, NRB outcompetes SRB due to nitrate being a stronger oxidizer than sulfate and thereby limits the generation of H_2S [134,139]. According to Little et al. [134], the SRB population was decreased, and NRB was increased; after a long-term period of 27 years of nitrate treatment, SRB numbers were reduced 20,000 times, and SRB activity was reduced 50 times [134]. Corrosion measurements decreased from 0.7 mm/yr to 0.2 mm/yr. Furthermore, another platform that has injected nitrate into its system to reduce H_2S production has reported a 1000 times reduction in SRB numbers, a 10–20 times reduction in sulfate respiration activity, and a 50% reduction in corrosion [134,137]. However, other researchers have reported failures related to the introduction of bacteria into natural mixed cultures. For example, Hubert et al. [140] suggested that bioaugmentation of NRB, which has grown *ex-situ*, was injected along with the nitrate batch if the presents of NRB were missing/low. Though, the considered idea failed regarding the injection of NRB along with nitrate batches. Another study by Xu [141] found that it is very likely that NRB corrodes the iron if there is a lack of carbon sources under the NRB biofilm [141]. The results by Xu [141] also revealed that pitting corrosion, caused by an NRB type (*B. licheniformis*), is more aggressive than a typical SRB under strictly anaerobic conditions.

Even though microorganisms are exposed to biocide and are not protected by biofilm, some microorganisms will still survive. Most organisms typically live in unfavorable environments where they experience conditions that are less than ideal for growth and reproduction [133]. A prevalent response to environmental stress for an organism to enter a reversible state of reduced metabolic activity and thereby going into dormancy (non-dividing state) [142]. From that perspective, some studies have even hypothesized that dormancy might be the default form of most microorganisms [143–145]. The dormancy defense mechanism protects the bacteria from exposing itself to unknown environments, where an antimicrobial agent could be present, which they are not resistant to [133,143]. This mechanism renders it challenging to analyze different microorganisms' metabolism *ex-situ*. It is notoriously difficult for process engineers to mimic the process in a laboratory, which may cause the selected biocidal agents to target unwanted activities.

The main types of microorganism associated with corrosion failures are SRB, iron/manganese-oxidizing bacteria (IOB) (also defined as metal-depositing bacteria (MDB) in other studies [118,146]), iron-reducing Bacteria (IRB) (also defined as metal-reducing bacteria (MRB) in other studies [118,146]), as well as slime-forming bacteria (SFB) and acid-producing bacteria (APB). Each type of microbial group that is associated with corrosion failures is described in the following subheadings. Some bacteria cultures can be categorized as different microbial groups, depending on the environment.

Slime-forming bacteria (SFB)

Metabolism: SFB covers a high amount of different bacteria [147]. SFB is a group of bacteria that is capable of producing a EPS, which acts as the foundation for the formation of biofilm. Many SFB fall within some of the other microbial groups [118,147]. **Formation damage mechanisms:** SFB has an indirectly influence of formation damage by promoting microbial growth inside the biofilm, attachment of other types of MIC, and development of *in-situ* ecosystem underneath a biofilm leads to formation of anodic and cathodic areas, promoting corrosion [148]. **Type ex:** *Vibrio cholerae*, as well as many other *Vibrio* spp., *Clostridium* spp., *Flavobacterium* spp., *Bacillus* spp., *Pseudomonas* spp., *Pseudomonas*, and *Aerobacter* [146,149,150].

Sulphate-reducing bacteria/archaea (SRB/SRA)

Metabolism: SRB are stated to be the most troublesome microbial group among MIC in the petroleum industry [151,152]. SRB and SRA, both of which primarily perform obligate anaerobic respiration, utilize sulfate (SO_4^{2-}) as a terminal electron acceptor and generate H_2S [120,137]. **Formation damage mechanisms:** Generation of H_2S , which souring the process and their activity is primarily realized as a pitting attack on the metal surface [118,137]. Some studies even observed plugging of the injection well by corrosion deposit flocs due to the increase of H_2S [152]. **Types ex:** *Desulfovibrio*, *Desulfobacter*, and *Desulfotomaculum* [149].

Sulfate-oxidizing bacteria (SOB)

Metabolism: SOB perform aerobic respiration. SOB can convert H_2S , that is produced by SRB, to H_2SO_4 [120]. **Formation damage mechanisms:** The generation of sulfate-producing acids, such as H_2SO_4 , are contributors to corrosion. If SRB and SOB are present these two type of groups almost always accompany each other, when the environmental conditions contains O_2 , it is suitable for the aerobic SOB, and vice versa [137,150,153]. **Type ex:** *Thiobacillus* spp., *Paracoccus*, *Xanthobacter*, *Alcaligenes*, and *Pseudomonas* [149].

Iron-reducing Bacteria (IRB)

Metabolism: Most of the IRB are facultative anaerobes. IRB influences corrosion by reducing insoluble Fe^{3+} oxide layer to soluble Fe^{2+} , or they replace the metal film on the pipeline surface with less stable metal film [137,146,154]. **Formation damage mechanisms:** Exposes the metal beneath corrosion deposits (Fe_2O_3) protective layer to a corrosive environment. IRB also makes the environment more suitable for SRB in a mixed population of microorganisms in the biofilm, as IRB consume the O_2 , and the SRB can thereby live under anaerobic conditions [137]. **Type ex:** *Shewanella* and *Pseudomonas* spp. [146,153].

Iron/Manganese Oxidizing Bacteria (IOB)

Metabolism: IOB form oxide and hydroxide mineral deposits that cover the metal surface and provide O_2 depleted zones where anaerobe microorganisms can propagate [153,154]. **Formation damage mechanisms:** Promote corrosion reactions by the deposition on the metal surface, which decrease or damage the the protective oxide films covered on the surface [118,146]. **Type ex:** *Gallionella*, *Leptothrix*, *Siderocapsa*, *Sphaerotilus*, *Crenothrix* and *Clonothrix* [118,146,149,153].

Acid-producing bacteria (APB)

Metabolism: APB can produce large amounts of acids as by-products during their metabolism, which can decrease the pH in the biofilm into a very acidic environment [118,146]. Production of inorganic acids can be HNO_3 , H_2SO_3 , H_2SO_4 , HNO_2 , and H_2CO_3 [118]. For example, H_2CO_3 can then further disassociate into CO_3^{2-} and CHO_2^- which can react with Fe resulting in the corrosion product FeCO_3 [153]. **Formation damage mechanisms:** Produce acids that causing metals to dissolve and accelerate corrosion processes [153]. **Type ex:** *Acetobacter*, *Gluconobacter*, *Pseudomonas*, *Thiobacillus*, *Thiothrix*, and *Beggiatoa* spp. [118,153].

Nitrate-Reducing Bacteria (NRB)

Metabolism: NRB reduce N_3^- to N_2 . As previously described, nitrate is often injected into the process to mitigate souring caused by SRB, as NRB can outcompete SRB and thereby reduce H_2S production. Studies proved that NRB efficiently oxidized the cathodic hydrogen from the metal, but unlike SRB cultures, they failed to stimulate the rate of corrosion [155]. **Formation damage mechanisms:** As previous described, corrosion caused by an NRB is more aggressive than SRB under strictly anaerobic conditions. **Type ex:** *Arcobacter*, *Bacillus licheniformis*, and *Desulfovibrio*.

3.6. Reflection

To summarize Section 3, it is essential to understand the different IW characteristics and their formation damage mechanisms on the IWT process if an acceptable online monitor for detecting TSS must be selected. For instance, if only considering TSS as inorganic particles and following the definition of TSS as particles above $2\text{ }\mu\text{m}$, then an operator could have a hard time troubleshooting why an increasing TSS concentration further down the treatment process occurs and determining which type of TSS increased the overall TSS concentration. The water quality can also be affected by substances like oil, clays, and TDS that have the ability to coalesce, agglomerate, swell, and change states, respectively. All particles that have the ability to pass the filters in the IWT process and changes conditions further downstream that could act to the measurements of TSS, both the size distribution and the concentration. Another example could be troubleshooting why there is an increasing replacement of corroded instruments if considering dissolved gases as the only stimulation of corrosion. Other issues are the performance of measuring OiW. Fjords Processing executed an extensive investigation of different online OiW monitors; some of the OiW monitors that are investigated are also able to measure solid particles. The results clearly indicated that all the OiW monitors were affected by some, if not all, of the parameter variations they were exposed to [156]. Most parameters must also be taken into account for a TSS monitor, such as particle size variation, the fluid carrier's flow rate,

salinity, oil, gas, chemical, temperature variation, and fouling. When monitors are installed in a field environment, a monitor will not be subject to all the different variations listed before if it is recalibrated regularly. Variations in TSS concentration and size distribution may change occasionally, where the flow rate and chemical concentrations change daily. How regularly the changes occur completely depends on the installation location and daily production. In an ideal situation, after the entire IWT process, the water quality, with respect to TSS, should output the same TSS concentration as after the last filtration unit in the IWT facility. Another aspect to consider is the location of measuring TSS in the process and what type of measurement method can output relevant information to monitor the quality of TSS in the IW.

4. Injection Water Treatment Facility

As IWT consists of various stages, it is important to understand each stage's purpose and its working principles. Especially with a focus on instrumentation of TSS monitor at different locations on the IWT facility and which physical process issues could affect TSS measurements. A current IWT facility in the Danish sector of the North Sea will be described as a benchmark. The salinity of seawater does not deviate seasonally around the IWT facility, with surface and bottom salinity of $\sim 3.5\%$, according to former Maersk Oil [157]. The surface temperature is around $7\text{ }^{\circ}\text{C}$ during winter and between 15 and $19\text{ }^{\circ}\text{C}$ in summer. The bottom temperature varies from 6 to $8\text{ }^{\circ}\text{C}$ in winter and 8 to $18\text{ }^{\circ}\text{C}$ in summer, where the temperature of the reservoir is typically $80\text{ }^{\circ}\text{C}$ [157,158]. As mentioned in Section 2, the mean TSS concentration in the North Sea is $2.6(3.5)\text{ mg/L}$ around Dogger Bank. The temperature increases through the process, and according to studies, the injection temperature outlet is often around $18\text{--}21\text{ }^{\circ}\text{C}$. Although, the temperature can easily increase with $10\text{ }^{\circ}\text{C}$ due to a higher injection rate, as the residence time in the subsea pipelines is shortened [158,159].

One of the primary problems in most injection systems, highlighted in several studies, is the entry of O_2 after the deaeration towers through leaking pumps, seals, hatches, etc. [26,99]. Inadvertently, contaminants may enter the system. The difficulty of preserving water quality is essential, and represents a direct function of the length and complexity of the injection system [26]. The results of water quality in long pipeline systems are often considerably worse than after the treatment source [26]. Figure 13 shows a block diagram of different process stages through an IWT system, where the process is described by Larsen et al. [158] and Thomsen et al. [159]. The main stages of IWT in Figure 13 are described in the following subheadings.

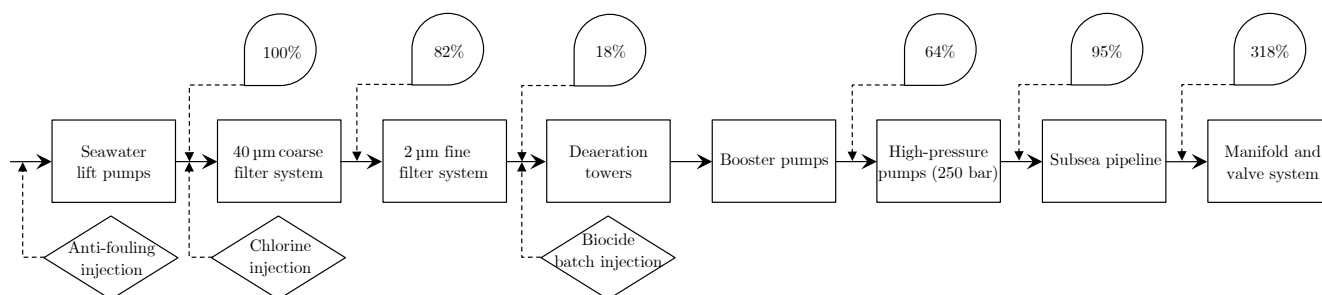


Figure 13. Block diagram of a water injection treatment facility in the Danish sector of the North Sea, with manual TSS concentration ratio at different locations on the IWT facility (exact concentration is confidential).

Seawater Lifting Pumps: A few pumps lift seawater from the ocean to the platform level. These pumps are often controlled by a constant speed; 3–5 pumps are often required. As the seawater is untreated at this point, the dispersed and dissolved content are highly reactive, thus requiring the pump and piping at these early stages to be highly resilient. Therefore, an anti-fouling agent is added before the lifting pumps to eliminate fouling for this particular benchmarked IWT facility.

Filtering: As solid particles are known to block pores in the reservoir, filters are utilized to remove sufficiently large solid particles. Chlorine is injected before the filter to protect the filters from biological fouling. At this time, there exist multiple solutions, but filtration systems might need improvements as the trend in oil and gas production is getting tighter, which involves injecting PW into the oil reservoir [160]. Some IWT solutions utilize a single-stage filter, where others use two-stage coarse and fine filters. Various types of filters are being used in the solution, such as cartridges, strainers, cyclones, membranes, and granular media types, where granular media types that define sand and nutshell filters are the most common [160]. As multiple of the same filter types are in use simultaneously in each train, it is of interest to divide the filter load equally among them as well as having an optimal filter cleaning procedure. The back-flushing cleaning procedure of the filters is commonly triggered by either exhausting a timer or after the delta pressure over the filter exceeds a limit [71]. It is also beneficial to balance the load between the coarse and fine filter states so that one stage is not redundant. As the continuous size distribution of the TSS is unknown, this load balance can be challenging to achieve [161].

Deaeration: As O₂ is unwanted in both the piping and reservoir, the concentration of O₂ in the water is reduced by deaeration. A common deaeration method is by tray-type vacuum deaeration towers. The operating principle of the trays is to increase the surface area and reduce the travel length of O₂. The deaeration towers' performance is currently measured by analyzing samples of the IW before and after deaeration. However, there are various reliability issues of these measurements as the concentration of O₂ in water should be low after deaeration. According to studies, the acceleration of corrosion occurs when the deaeration O₂ content of the water is above 0.025 ppm [99,100]. The concentration of O₂ in the samples might change over time, from sample extraction to sample analysis, which causes errors when evaluating the performance [100].

Injection Pump, Manifold, and Valve Systems: The booster pumps raise the pressure to 10–16 bar before the injection pumps raise the pressure to around 250–300 bar [158,159]. The IW is then either directly injected into the nearest wellheads or transported through a ~10 km long subsea pipeline, and some of the IW is even further transported ~2 km to another wellhead, where it enters the last part before injection into the reservoir [158,159].

4.1. Total Suspended Solids Dried Weight Measurements

As different IW characteristics and their formation damage mechanisms on an IWT process are well described in Section 3, followed by a description of how a specific IWT facility is constructed to purify the IW before injection, it is of interest to investigate the location of where online TSS monitors can be beneficial to install, and which type of method, size range, and type of matters the monitor have to measure. Furthermore, it is also necessary to determine how the measurements can be useful to increase water quality. As the exact TSS concentration are confidential in Figure 13, a manual experiment of emulating the filtration system was executed. The measurement of TSS followed the Danish standard for “Dry Weight and Loss of Ignition Analysis”, which are closely related to the American standard for Total Suspended Solids Dried at 103–105 °C [64,162]. The concentration of TSS is calculated as

$$X = 1000 \cdot \frac{(b - a + c)}{V}, \quad (4)$$

where c is the blank sample's weight loss after drying:

$$c = \frac{a_0 - b_0}{3}. \quad (5)$$

The rest of the variables are a is the weight of the unused filters [mg], a_0 is the weight of three unused filters for blank sample [mg], b is the weight of the dried blank sample filters with suspended solids [mg], b_0 is the weight of the three washed and dried blank

sample filters [mg], and V is the filtered amount of volume [ml]. The three different filters used for determining the concentration of TSS in a specific area and depth in the Danish sector of the North Sea were

- **41 μm filter:** Nylon filter—Sepctral/Mesh[®] Woven Filters—follows the U.S.A standard sieves ASTM specification E-11 for a mesh with a permissible variation of $\pm 3 \mu\text{m}$ for a 41 μm filter [163];
- **2.7 μm filter:** Glass Microfiber filters—Watman[™] 1823-047 Grade GF/D—Particle retention rating at 98% efficiency [164]; and
- **0.2 μm filter:** Mixed Cellulose ester—Advantec[®] Membrane filters.

The 41 μm and 2.7 μm filter are used to emulate the two different filtration processes on a specific IWT system. The 41 μm filter emulates the 40 μm coarse filter system, and the 2.7 μm filter emulates the 2 μm fine filter system that is installed on the IWT system. The 0.2 μm filters are used to retain anything that passes the two emulation filters and is defined as the “TSS sample” in Figure 14a.

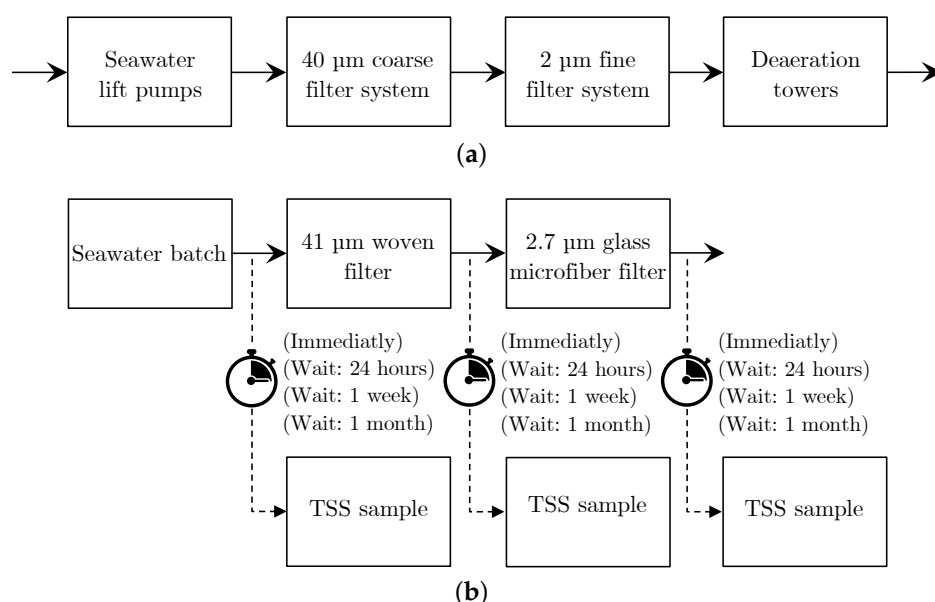


Figure 14. Two flow diagrams of the filtration process offshore and emulation in laboratory: (a) The filtration sections of benchmark IWT process offshore, cf. Figure 13 to see the entire flow diagram of the IWT process. (b) An emulation of the filtration process, where seawater from the intake to the offshore process is collected and tested in laboratory. The seawater is filtered through 41 μm filter and a 2.7 μm filter, to emulate the filtration process offshore, between each filtration a TSS sample is retained by vacuum filtration through a filter with pore sizes of 0.2 μm . The TSS samples are analyzed at four different time periods: immediately, after 24 h, after one week, and after one month.

The 0.2 μm filters are selected as, ideally, no microorganisms nor inorganic particles should pass the filter. The TSS samples are analyzed at four different periods: immediately, after 24 h, after one week, and after one month, as shown in Figure 15.

By looking at the future development to test the null hypothesis (H_0) if any evolution of microbial growth has occurred in the seawater after preservation and transportation onshore for analysis. The analysis of variance (ANOVA) test of the samples between each filtration analyzed at different periods does not statistically show any significant evolution, and the H_0 can be rejected, and the means are likely to be equal for all periods. The ANOVA results are listed in Table 3 for each filtration group.

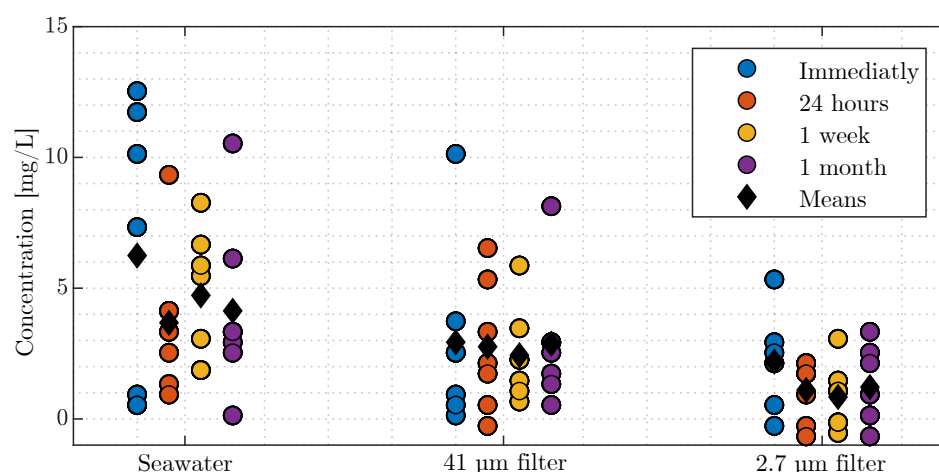


Figure 15. Scatterplot of each sample analyzed at the four different periods.

Table 3. The ANOVA test results of each sample location at the four different time periods: immediately, after 24 h, after one week, and after one month.

Unfiltered seawater					
	SS	df	MS	F-value	P-value
Between groups	26.35	3	8.78	0.64	0.60
Within groups	329.78	24	13.74		
Total	356.14	27			
41 µm filter					
	SS	df	MS	F-value	P-value
Between groups	1.03	3	0.34	0.05	0.98
Within groups	162.93	24	6.79		
Total	163.95	27			
2.7 µm filter					
	SS	df	MS	F-value	P-value
Between groups	7.32	3	2.44	1.18	0.34
Within groups	49.55	24	2.06		
Total	56.87	27			

This concludes that preservation of the seawater prevented the growth of microorganisms, and a joined boxplot for each filtration group can represent the TSS concentration, see Figure 16.

The mean seawater TSS concentration from the experiment reflects the TSS concentration according to the study of 2.6(3.5) mg/L by Prandle et al. [31]. The mean and standard deviation for each filtration of the measured TSS concentration is estimated to be as follows.

- Unfiltered seawater: 4.7(3.6) mg/L
- 41 µm filter: 2.8(2.5) mg/L
- 2.7 µm filter: 1.3(1.5) mg/L

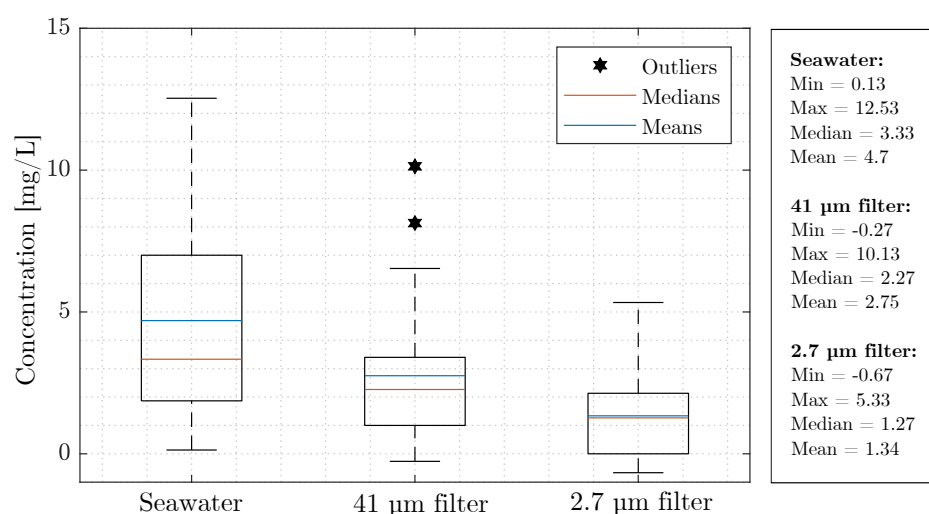


Figure 16. Shared boxplot representation of between each filtration: unfiltered seawater, 41 µm filter and 2.7 µm filter.

The executed TSS concentration value can be used to compute a hypothetical value of the TSS concentration evolution throughout the IWT facility, based on the TSS concentration ratios expressed in Figure 16. Table 4 shows the measured TSS concentration compared with the expected TSS concentration, assuming the mean and standard deviation from the literature of 2.6(3.5) mg/L. The expected TSS concentration from literature is calculated according to the percentages presented in Figure 13. Measured TSS concentration is based on measured concentration from Figure 16 and subsequently calculated as percentages.

Table 4. Comparison between the measured TSS concentration and the expected TSS concentration from the literature: 2.6(3.5) mg/L.

	Expected TSS conc. [%]	Expected TSS conc. [mg/L]	Measured TSS conc. [%]	Measured TSS conc. [mg/L]
Seawater lift pumps	100	2.6(3.5)	100	4.7(0.6)
Coarse filter system	82	2.1(2.9)	60	2.8(2.5)
Fine filter system	18	0.5(0.6)	28	1.3(1.5)
Booster pumps	64	1.7(2.2)		
High-pressure pumps	95	2.5(3.3)		
Subsea pipeline	318	8.3(11.1)		

The TSS concentrations in Table 4 are in reasonable relation between measured and expected TSS concentration through the system. There could be a substantial uncertainty related to the fact that the expected TSS concentration is calculated based on percentage, but it is assumable that both TSS concentrations are within the expected range. With nearly a 17-fold increment of the mean after the fine filter system to after the subsea transportation pipeline, it clearly indicates the addition of TSS such as scales, corrosion deposits, and microbial grows, assuming the filtration systems works as intended. This also concludes that the instrument of monitoring the particle size distribution should be measurable within an overall TSS concentration from >30.5 mg/L ($\mu + 2\sigma$) to ~ 0 mg/L. As an increasing amount of TSS is added within the process, it is difficult to conclude the actual size of particles based on the TSS concentration results.

5. Online Monitoring Total Suspended Solids

Online measurement of TSS requires proper calibration and regular maintenance, like many other continuous measurement devices. Extensive development in the area of implementation of process analytical technology of measuring particle sizes has been investigated for decades. Despite the long history of implementing quality monitors for

measuring particle sizes, it has not become a standard operation parameter in the oil and gas industry. However, measuring particle sizes continuously is highly essential to increase the performance of IWT processes. It is evident that the particle size distribution significantly affects the quality of the reservoir. Nevertheless, the trustworthy particle size distribution of TSS and their shapes also affect the process control, and can be valuable to validate the IWT process design.

In general, TSS monitors work well when they are properly calibrated and well maintained in non-hazard environments. However, in the oil and gas industry, significant variations of mixtures, pressures, chemicals, and temperatures render a harsh environment for the online TSS monitors, all of which influence the accurate measurement of the particles in the process. In many cases where the monitors have been installed without proper calibration, maintenance, or actual knowledge of the limitations of the installed monitors, doubtful and misleading results have resulted [165]. As described in Section 3, the operators must have confidence in the data generated by the monitor, as action misled by inaccurate measurements can cause more harm than not taking any action at all. Several commercially available monitors exist for detecting oil droplets and particle sizes, with different measurement techniques, ranging from technologies based on ultrasonic spectroscopy to electrical sensing zone. However, no commercialized monitors have been standardized for detecting TSS or OiW continuously to the authors' knowledge.

Currently, different international or industry standards, such as International Organization for Standardization (ISO), American Society for Testing and Materials (ASTM), and American Petroleum Institute (API), covers different focus area, ranges, and analysis methods. A new monitor must be compared with the right standard for validating its performance, which on its own can be difficult. Tables 5 and 6 contain the ISO standards related to measuring particle sizes suspended in liquid, that includes definitions, discrimination of different type of TSS, representation, sampling, as well as the technical characteristics and working principles of the most common particle sizing instruments.

Table 5. ISO standards for representation of particle size analysis results and related standards.

	ISO Standard(s)
Representation of particle size analysis results:	
Graphical representation	9276-1
Calculation of particle size distribution	9276-2
Adjustment of an experimental curve to a reference model	9276-3
Characterization of a classification process	9276-4
Size analysis using logarithmic normal probability distribution	9276-5
Representation of particle shape and morphology	9276-6
Repeatability, reproducibility and trueness estimates	21748
Other standards of interest:	
Determination of suspended solids	11923
Manual sampling	3170
Automatic pipeline sampling	3171
Preservation and handling of water samples	5667-3
Determination of turbidity	7027
Microbiological examinations by culture	8199
Oil-in-Water concentration	9377-2
Particulate materials—Sampling and sample splitting	14488

Table 6. Relevant ISO standards for particle size analysis methods.

Particle Size Analysis' Methods	ISO Standard(s)	Overall Size Range [μm]	On-/In-Line Capable
Sieving	2591-1	5–125 *	X
	3310-1 to -3		
	20977		
Gravitational sedimentation	13317-1 to -4	0.5–100	X
Centrifugal sedimentation	13318-1 to -3	0.1–5	X
Electrical sensing zone	13319	0.4–1200	✓
Laser diffraction	13320	0.1–3000	✓
Image analysis methods	13322-1 to -2	(0.3)/3–500 *, **	✓
Small-angle X-ray scattering	17867	0.001–0.14	X(✓)
Scanning electron microscopy	19749 ***	0.01–500 *	X
Ultrasonic attenuation spectroscopy	20998	0.01–3000	✓
Transmission electron microscopy	21363 ***	0.001–5 *	X
Light obscuration	21501-3	1–100	✓
Dynamic light scattering	22412	0.005–1 *	✓

* No typical size range was given within the ISO standards, found according to Merkus [166]. ** The overall size range cover only light microscopy. *** ISO standard under development.

As there does not exist one unique reference method for measuring particle sizes, it can be difficult to verify the performance of different measurement techniques. The TSS concentration can be measured and compared according to the ISO 11923 reference method by a filter, drying and weighing the water sample; the same procedure as executed in Figure 16. However, it tells nothing about the particle morphologies in the process.

Currently, offshore IWT processes utilizes manual measurements for TSS concentration. The measured quantities can vary under different operational conditions and between different laboratories. The reference method is also limited in detecting all quantities defined within TSS. As a consequence, a very detailed procedure for taking a sample, transportation, storage, and measuring in a laboratory is well described in ISO 5667-3, for manual sampling (ISO 3170), which makes the measurement of TSS not only method-dependent but also procedure-dependent [10]. Even though the reference method for TSS concentration is a well-defined procedure, the method- and procedure-dependency introduces a substantial amount of uncertainties. Therefore, it can be difficult to validate and compare the performance of the process and achieve confidence in new measurement techniques [10,167].

In the ideal world of particle characterization, all particle size analysis methods within their recommended measurement range, highlighted in Table 6, should yield an unambiguous diameter size of particles under the condition that particles are spherical and homogenous distributed (constant concentration). Moreover, their chemical composition should be identical, as different properties, such as density, refractive index, and conductivity, would affect the different methods [166]. Even so, the concentration of particles can still affect the output from different measurement techniques. It would be apparent that such ideal conditions of particle sizing would ease the establishment of defining a reference method. It is also clear that most particles have irregular shapes and chemical composition in the real world and are not homogeneously distributed in the sample. These differences all have different influences on different measurement techniques. Some are more robust to high sample concentration than others (ultrasonic compared to electrical sensing zone), some have entirely different measurement ranges than others, and some are cable of measuring on-/in-line. Based on measurement ranges and installment capability, it is possible to discriminate which method is suitable for measuring TSS online.

The different automated methods of detecting particle size distribution (PSD) have increased considerably in the last decades, especially due to the increment of computation power and the fact that almost all operating plants in all fields are today entirely controlled automatically. Even with increasing sophistication within each measurement technique, there is still an urge to improve accuracy and increase resolution. There are numerous

particle size analysis methods, each with different approaches. Thus, each has its theoretical interpretation and different analyzing procedure of the same particle (spherical or non-spherical shaped). Another drawback, related to the different measurement techniques, is the fact that all non-spherical particles are assumed to be spherical [166–168]. Different technologies will yield different PSD, based on the exact same sample as most methods do not include particle shape information [166,169].

5.1. Particle Size of Measurements

In this section, the ISO definition of particle size measurement is introduced briefly, as a more in-depth description can be found in the ISO standards; highlighted in Table 5. Understanding these uncertainties and the sensitivity of these TSS monitors is a prerequisite for successful implementation and comparison of different measurement techniques. Such an understanding could lead to an improved combination of different monitors' technology methods through sensor fusion. More technical descriptions of particle size analysis have been well described, discussed, and compared in different studies [166,169–171]. Some of the most common particle size measurements, as highlighted, quantify particle sizes differently.

Spherical particles only require to be represented by one parameter; their diameter. For any non-spherical particles, this can only be approximated by an equivalent diameter; otherwise, more size parameters are needed. Equivalent diameter is defined as the diameter of a spherical particle, which yields the same value of a certain physical property when analyzed under the same conditions as the non-spherical particle [172]. According to ISO standard 9726-2, there are different physical properties that characterize particles:

- linear dimension;
- projected area;
- surface area;
- volume;
- mass;
- settling rate; and
- the response of electrical, optical, or acoustical field.

Each of these properties can be used to characterize the equivalent diameter of a particle. The isoperimetric quality is only valid if the particles are spherical, as spheres have the largest volume to surface area ratio with a non-empty inner body [173]. The equivalent projected area diameter is the diameter of a sphere having the same projected area as the particle. That is often the case for particle size analyzers, as the particle has a specific orientation when passing the monitor, such as microscopy and light scattering. The equivalent projected area diameter of a particle, d_A , can be calculated equivalent to circle area:

$$d_A = \left(\frac{4A}{\pi} \right)^{1/2}, \quad (6)$$

where A is the projected area. Depending on the orientation of the particle, d_A can both be smaller or larger compared to the other equivalent diameters in a continuous flow stream.

The equivalent surface diameter, d_S , and volume diameter, d_V , are based on the three-dimensional geometry of a single particle. The equivalent surface diameter is calculated based on a sphere having the same surface area as the particle:

$$d_S = \sqrt{\frac{S}{\pi}}, \quad (7)$$

where S is the particle surface area. Similarly, the equivalent volume diameter is calculated based on a sphere having the same volume as the particle:

$$d_V = \left(\frac{6V}{\pi} \right)^{1/3}, \quad (8)$$


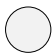
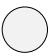
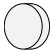
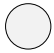

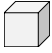




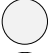


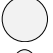
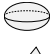
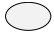
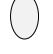


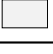
where V is the particle volume [174]. For non-porous particles consisting of one material, the mass equivalent diameter, d_M , is equal to d_V . Stokes equivalent diameter, d_{St} , corresponds to the diameter of a sphere with the same final settling velocity as the particle in Stokes regime with the same density, defined by Stokes' law:

$$d_{St} = \sqrt{\frac{18\mu v_t}{g\Delta\rho}}, \quad (9)$$

where v_t is the settling velocity, g is the acceleration due to gravity, μ the dynamic viscosity of the carrier liquid (IW), and $\Delta\rho$ are the densities of the carrier liquid and the particle. Last, the equivalent sieve diameter, d_{sieve} , corresponds to the diameter of a sphere passing through a defined square sized mesh. These are the most frequently used analyze methods of representing a particle size with only one size parameter. Other methods to quantify the particle size exist, especially for microscopy analysis, e.g., Feret diameter, Martins diameter, and convex perimeter.

The relationship between particle analyzers using equivalent diameter to represent particles' size is very important to address, as a comparison of different analyzing equipment using a different physical property to characterize particles can give different distributions. Thus, care should be taken if one compares the data from a different type of analyzing equipment and expect related outcomes. Table 7 gives a theoretical analysis of the outcome by obtaining different equivalent diameters on several convex particles having the same volume of $V = 1000 \mu\text{m}^3$, together with its relative value compared to a sphere.

Table 7. Theoretical characterization of different convex particles based on different physical properties.

Shape	3D ill.	Orientation		Dimensions: $d, d \times h,$ $l \times w \times h [\mu\text{m}]$	$d_A^* [\mu\text{m}]$		$d_s [\mu\text{m}]$	$d_{St}^{**} [\mu\text{m}]$	
		O_1	O_2		O_1	O_2		O_1	O_2
Sphere				12.4	12.4	12.4	12.4	12.4	12.4
Disc				25.2×2.0	25.2	8.0	19.2	31.8	8.6
Rectangular prism				$7.0 \times 7.0 \times 20.4$	7.9	13.5	14.6	10.1	18.1
Cone				19.5×10.0	11.1	19.5	15.2	12.7	24.0
Cylinder				8.0×20.0	14.3	8.0	13.9	15.8	8.3
Ellipsoid				$12.0 \times 10.6 \times 15.0$	11.3	12.6	12.5 ***	11.2	12.8
Triangular prism				$10.0 \times 10.0 \times 20.0$	8.0	16.9	16.4	9.2	21.2

* d_A and d_{St} are obtained at two orientations: O_1 and O_2 . ** The drag force of spherical and non-spherical particles is calculated according to the drag prediction approach presented by Ganser [175], where the drag coefficient for a sphere is estimated to be $C_d = 26.7$ at $Re = 1$.

*** Knud Thomsen's approximation of an ellipsoid surface area with a worst error of $\pm 1.061\%$.

In summary, equivalent diameters are still necessary information to calculate for measuring the PSD in processes, especially in a process where the particle of interest is the majority, e.g., measuring the oil droplets from PW treatment processes.

5.2. Instrumentation

Each measurement technique can be divided into online methods that deliver data in a process-relevant time window and manual methods. A further subdivision of the measurement methods can be made on the sampling point: in-line, on-line, at-line, and off-line, see Figure 17.

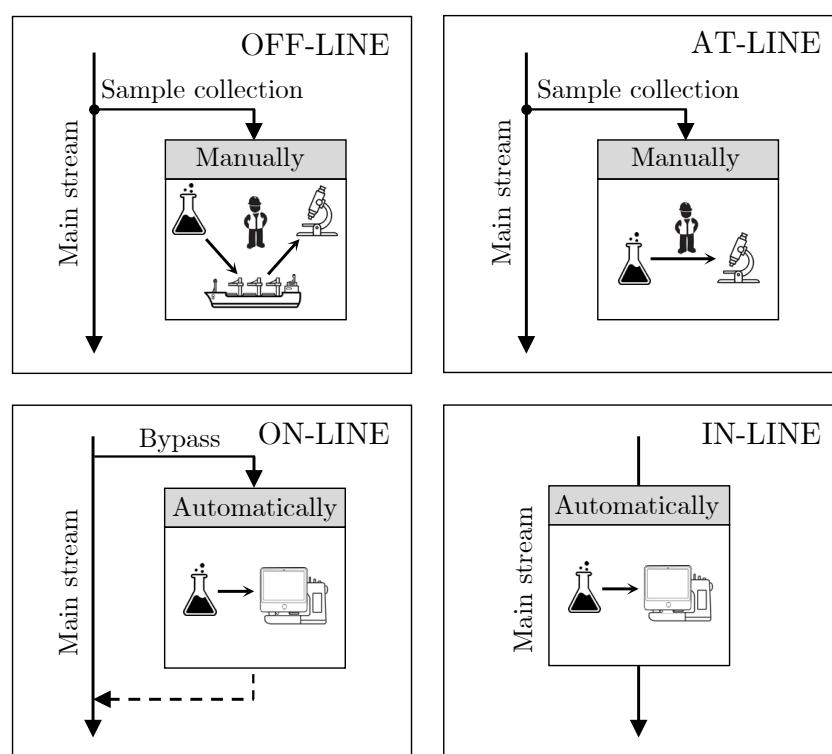


Figure 17. Different sampling methods based on the sampling point: in-line, on-line, at-line, and off-line.

Off-line analysis advantages in the manual examination of the sample are carried out by experts in laboratories. The sample preparation is adjusted to suit the particular method of analysis and types of quantities being examined. For off-line analysis offshore, the sample needs to be prepared (i.e., diluted, mixed, and preserved) to reduce changes under transportation, and a substantial number of samples are needed to verify the trueness of the measurement, which renders it a time-consuming process. Especially at offshore processes, it can take several days, if not weeks, between sampling collection and the results, obtained onshore. For this reason, feedback from the laboratories to the platform has a significantly longer reaction time, which is accentuated when a noteworthy deviation occurs due to faults of the production or, even worse, process damage.

At-line analysis deviates from off-line analysis by carrying out the sampling analysis closer to the process. Like off-line analysis, at-line analysis is still a manual procedure that demands human resources compared to fully automated analysis procedures as on- and in-line analysis. The at-line location reduces the amount of preparation for transportation. Unlike off-line analysis, the closer proximity to the process also considerably reduces the reaction time, which could have a valuable effect on detecting adverse conditions earlier. Compared to off-line analysis, the disadvantage is that it may not be an ideal environment due to varying conditions, such as air humidity, temperature, and cleanliness.

On-line analysis differs from the off-line and at-line methods as the sampling is automatic, which significantly reduces the reaction time of analyzing the quality of the IW. The automatic analysis guarantees the possibility of reacting promptly to any deviations from normal operation. To clarify, online monitors can be installed in both on-line and in-line configurations. TSS measurements have the potential to be used as feedback for improving process control. The disadvantage of on-line analysis, like off-line and at-line, is the risk of a bypassed maldistribution of the heterogeneous mainstream, which may not represent the true process quality. Manual sampling analysis is still necessary to verify the measurement quality of the TSS measurement equipment.

In-line analysis and on-line analysis are closely related and share some advantages and disadvantages. An in-line analysis is done *in-situ* of the process stream directly. Thus, no misrepresentative sampling due to bypassing the flow happens nor disturbances in the process stream. However, the in-line analysis does have some disadvantages; the equipment must be robust within its procedure to prevent shutdowns from carrying out an inspection.

5.3. Particle Size Analysis Methods

Several particle size analysis' methods listed in Table 6, can be discriminated due to the application of measuring on-/in-line with an ideal upper limit of $>40\ \mu\text{m}$ to determine whether the coarse and fine filters are malfunctioning and a lower limit of at least $<2\ \mu\text{m}$ to determine the filtration quality. Based on those criteria, the techniques that are applicable for detecting concentration and particle sizes in IW are electrical sensing zone, light scattering, light obscuration, ultrasonic spectroscopy, microscopy, and turbidimetry. Although turbidimetry itself does not have the possibility to measure particle sizes, it is commonly used for measuring water quality. The accuracy of each method, described in different fields of installation, will not be mentioned in this paper as the results may be tendentious. A short description of each method will be given with their advantages and disadvantages, with respect to measuring TSS in IW.

Turbidity method (Turbidimeters):

Turbidity monitors are commonly used in water industries. Turbidity monitors measure the intensity of scattered light due to particles within the water that disrupt the transmitted light path [176]. The detector then measures the scattered light as the light changes direction when it hits the particles. The light energy is then converted to an electric signal, which outputs a calibrated nephelometric turbidity unit (NTU) value, i.e., if the water is less turbid, less light is scattered, and thereby low output of NTU. The sensitivity of turbidity monitors may differ between instruments, but ideally, all types of particles, such as silt, clay, algae, organic matter, and microorganisms, scatter light in water [177]. One of the most significant advantages of turbidimeters is the sensitivity to particles below $1\ \mu\text{m}$ in size, all of which can contribute to the overall turbidity value [178]. However, care should be taken if comparing turbidity measurement with TSS concentration, as turbidity is another parameter of measuring water quality. For instance, turbidity also depends on particle sizes, bubbles, color, organic matter ability to absorb light, and type of microorganism, all of which affect the correlation between turbidity measurements and TSS concentration [177,179,180]. Other conditions can affect the measurement, such as the light scattered by particles at the back of the sample volume, which can be blocked by particles closer to the detector [178]. It is well known in the field of turbidimeters that bubbles affect the turbidity measurement, where particles identical in size, but have different chemical composition, scatter different amounts of light [178]. Even some organic matter, such as colored dissolved organic matter (CDOM), can result in an artificially low turbidity measurement as it absorbs light instead of scattering it [179,180]. Nonetheless, it may be unreliable to use turbidimeters for measuring the true TSS concentration, but their strength of measuring the water's turbidity may have the potential in combination with other water quality monitors [178].

Electrical Sensing Zone Method (Coulter Counter):

This instrument was initially developed for sizing blood cells and cell cultures and is widely used for off-line measurements [166,170,171]. The electrical sensing zone (ESZ) method relies on the impedance measurement in a capillary, through which particles within the IW (electrolyte) pass through a small orifice. When particles pass through the measuring gap, they momentarily change the electrical impedance equal to its volume of electrolyte [170]. This change in impedance generates voltage pulses corresponding to the number of particles, whereas the amplitude of the pulse is proportional to the volume of the particles and is used to measure the equivalent volume diameter of the

particle. The ESZ method excels in its high sensitivity and that it is capable of measuring a truly volumetric value of a single particle relative to other methods. Nevertheless, its disadvantages for installation in an IWT process surpass its advantages. The size range of particles is governed by the orifice diameter, where the overall size range is about 0.4–1200 μm [169].

The lower measurement limit depends on both electric noise and orifice size. Normally, particles with diameters ranging from 2% to a maximum size of 40–60% are noted by different studies to be reliably detected [64,166,170,171,181]. The signals of smaller particles are lost due to the signal-to-noise ratio; particles larger than 40–60% give an increasingly nonlinear response and can physically block the orifice [166,170,181–184]. The selected orifice diameter can then be estimated based on the particle sizes. As previously concluded in Section 4.1, for an IWT process, it could be of interest to measure from small micron sizes to very fine sand (4ϕ). The lower limit sets the orifice size, i.e., if 0.4 μm should be 2% of the measurement range, the orifice diameter will be 20 μm , with a reliable measured size range of 60%; 0.4–12 μm or for 40%; and 0.4–8 μm . Although an upper limit of TSS sizes of 8–12 μm should be enough to detect particles after the fine filter, changes can occur after the filtration unit that may frequently block the ESZ instrument further down the IWT process due to different mechanisms described in Section 3. Another drawback is that the method cannot distinguish between droplets and different particles [185]. Furthermore, only one particle at a time can be measured accurately within the sensing zone. Two types of coincidence can be distinguished [170,178,181].

- Primary Coincidence: more than one particle in the sensing zone gives rise to two or more individual pulses which cannot be distinguished and are overestimated as one particle and lower the particle counts.
- Secondary Coincidence: two or more particles below the detectable threshold level, which individually should not be detected, generate a pulse above the threshold level together. Thus, larger numbers of small particles are counted and overestimated [170,181].

Both coincidences increase the higher the concentration is, and the measured concentration should not exceed around 10 ppm, according to Merkus [166], although it is highly dependent on the presence of different types of particles. Last, for particles with an extreme shape, i.e., thin plates and needles, a large overestimation can appear as the particle may rotate when they are passing the sensing zone, creating an artificial measured volume [170,182].

Static Light Scattering method (Laser Diffraction):

Static light scattering measures the intensity of light scattered by the particles passing a beam of light. Static light scattering, which is sometimes also referred to as laser diffraction, or low-angle laser light scattering, is a well-established technology that has been used for decades for particle size analysis [55,171]. The scattered light that interacts with the particles is captured by photodetectors, which converts scattered light to an electric signal. Larger particles scatter the light more strongly but with lower angles than smaller ones, which scatter the light more weakly and with a larger angle, assuming identical matter [178,186]. Its advantages include being a well-established method, and its principles and limitations are well described in several textbooks. Light scattering sensors do also have an advantage in their sensitivity; their overall range spans from 0.1 to 3000 μm depending on the used instrument design and algorithm, which covers the TSS range of interest in an IWT process [64,166]. However, it can be difficult to distinguish between species present in a distribution, such as oil droplets, solid particles, and gas bubbles. Like many other particle analyzers, light scattering monitors assumes particles to be spherical. For non-spherical particles, the diameter of the particle is equivalent to the amount of light scattered, which depends on particle orientation. For platy- and needle-like particles, it often results in an overestimation of their sizes [170]. The scattered light pattern resulting from hitting non-spherical particles can vary as a function of the particle sizes,

shapes, refractive index, and scatter angle. The conversion from the angle and intensity of scattering to particle size is determined based either on the principles of Fraunhofer diffraction or Mie scattering theory [64]. Algorithms based on Mie scattering theory should ideally be applied for particles below a range of 25 μm or 50 μm , according to different studies [166,182,187]. The Mie theory requires the knowledge of refractive indices, which are mostly not available of organic matter and not directly measurable when passing the instruments beam of light [182]. Thus, it practically problematic to use in the IWT process if striving for accurate PSD [182]. Alternatively, some light scattering instruments extend the lower limit of the Fraunhofer diffraction algorithm, which does not require the refractive index, by collecting the scattered measurements from two or three wavelengths of incident light at a fixed angle [64].

Light Obscuration Method:

Light obscuration is another method of using light for measuring particle sizes. Light obscuration, also referred to as light blockage or light extinction, measures the diametrical opposite compared to light scattering. Light obscuration measures the light absorbed or reflected away from the photodetector in the sensing zone by the particle. The obscuration of a particle then decreases the photodetector's intensity generating an electric pulse [181]. Depending on the particle size, larger particles will intuitively block more light [178]. It delivers a measurement of size ranges usually from 1 to 2 μm and above [64,170,178]. Like ESZ, for accurate counting, only one particle must be present in the sensing volume due to the same reasons described for the ESZ method [181]. Light obscuration particle counters differentiate from the ESZ method for determining particle sizes, as the method only measures in the two-dimensional plane. Thus, the particle size is determined based on the projected area and not the volume. Light obscuration excels in being less affected by variations in the relative refractive index compared to light scattering [170]. As an example of this, assume two different particles of identical size that pass through the sensing zone of both methods. One particle is crude oil, and the other is stainless steel. Due to their different refractive indices, the particle of stainless steel will reflect considerably more light than the particle of crude oil [170]. Both types have their difficulties when particles refract light as the refracted light passes through the particle, i.e., a microorganism, which is almost transparent [178,186]. Its disadvantage, compared to light scattering, is the lower sensitivity.

Ultrasonic Spectroscopy:

Ultrasonic spectroscopy, also referred to as ultrasonic attenuation or acoustic spectroscopy, is a relatively new technique that has emerged in the last couple of years for online PSD analysis [166,170,186,188,189]. It is considered to have the potential for higher accuracy and feasibility beyond methods using light [170]. Its main advantages are the ability to penetrate opaque systems and still be noninvasive and non-intrusive in its way of measuring [166]. Furthermore, the ultrasonic methods typically make measurements over a range of 1 MHz to 200 MHz, which enables them to cover a wide range of particle diameter, from 10 nm to millimeters [189,190]. The measurement principle is based on ultrasonic waves travel through a sample material at different frequencies. All particles that pass through the measurement volume then transmit, reflect, absorb, or scatter the acoustic energy, equivalent to light methods. Thus, by measuring both the wave velocity and attenuation caused by the particles' morphology, the PSD can be estimated [188,189]. The ultrasonic velocity is the distance the ultrasonic wave moves through the sample per unit time, whereas the attenuation coefficient is a measure of the decrease in the amplitude of the ultrasonic wave per unit distance traveled [190].

The sound attenuation can be deployed in different ways: continuous waves, tone burst, or broadband pulses, all of which have shown their ability to give an estimate of the PSD [188]. The frequency spectrum of the transmitted ultrasonic signal can then be obtained by the application of fast Fourier transform (FFT) [186,191]. There are two approaches to

gain the measured signal: through-transmission and pulse-echo. The through-transmission mode receives the ultrasonic signal on the opposite side of the sample volume. In comparison, the pulse-echo mode receives the reflected signal on the same side as the signal excitation [191]. The difficulty of using ultrasonic spectroscopy lies in developing a proper model for determining the complex interactions between ultrasonic waves and particles' properties, for calculation of the accurate particle size and classification [188,189]. Despite its advantages, it has some technical issues that must be addressed. Mostly, particles are assumed spherical, and the presence of small gas bubbles also obscures the signal in ultrasonic spectroscopy as they strongly scatter ultrasound [190]. Ultrasonic measurements also require knowledge of different thermophysical properties of the dispersed and continuous phases to interpret ultrasonic spectra, such as density, thermal conductivity, thermal expansion, viscosity, speed of sound in the continuous phase, and heat capacity [189]. Most properties might be known reasonably well for the continuous phase (IW) in the process, but it can be challenging to estimate for the dispersed phase (TSS) [189,190]. McClements [190] concludes that it is necessary to develop a database of the relevant thermophysical properties commonly observed in the dispersed phase of the process [190]. The database is also necessary for further classification of each particle. Even though it is possible to distinguish between oil droplets, solid particles, and gas bubbles, it is not straightforward, according to Zhang [192]. Most of the disadvantages may be solved in the near future as the technology is a less-established measurement technique for measuring particle sizes, and only a limited number of ultrasonic-based field applications are known in the oil and gas industry (i.e., Mirmorax).

Microscopy and Image Analysis:

Automated digital microscopy analysis of images differentiates between static and dynamic analysis. In static image analysis, images of the solution are captured by dispersing the solution onto a surface for analysis. As the particles are analyzed on a surface, they settle at a stable state and often orientate their largest projection area to the camera. Regarding static image analysis, it is often related to manual sampling or automatic at-line analysis based on integrated algorithms to analyze the solution. Instead, in relation to online measurements in processes, dynamic microscopy analysis of images is used in both on- and in-line installations [169]. Digital microscopy utilizes a high-resolution video camera to capture images of the sample stream [55]. The 2D projection of the particles is then digitalized by conversion into pixels. The most common type of microscope used is called "bright field", as it forms a dark image of particles in focus with a bright background. The resolution of a microscope is a function of the optical magnification, focus quality, numerical aperture, type of immersion media, and also optical characteristics of particles (e.g., bacteria can be difficult to capture with bright field due to being opaque). The fundamental formula expresses the theoretical limit of resolution of a microscope:

$$d_0 = \lambda / 2NA, \quad (10)$$

where d_0 is the shortest distance between to measured points, λ is the wavelength of light used to capture the image, and NA is the numerical aperture. Using visible light closes to near-ultraviolet light (shortest wavelength) gives the highest resolution in the visible light spectrum; green light is often used as the visible light spectrum is centered at about 550 nm, and an oil immersion objective lens with an $NA = 1.45$, then the (theoretical) limit of resolution is 190 nm [193]. Consequently, particles in closer proximity than 0.2 μm appear as a diffuse point, and their size will consequently be overestimated. The exact limitation for measuring the smallest particle size, with a given accuracy, should be specified by each individual manufacture, but usually, the smallest particle that is targeted is around 1–2 μm , as smaller particles are limited by the number of pixels that represents the particle. Through image analysis, particles are then identified and counted, and different geometric or physical properties can be calculated, such as the particle size, shape, and volume. For spherically shaped objects, such as droplets or bubbles, the size of the particles can

easily be calculated, such as Feret diameter or equivalent area diameter. Both oil droplets and gas bubbles are spherical but can be distinguished due to the differences in their optical properties [55]. Microscopy analysis has its advantage over other methods as being a direct method; it can include shape information. Based on the included software they can classify each particle based on the measured parameters.

Even though microscopy image analysis can measure more parameters than indirect methods, it is still challenging to transfer the image's parameter information into meaningful values. Therefore, particle sizes are often represented as equivalent diameter, though it can measure both the width and height of particles. It even can represent other equivalent diameters than based on the projected area, e.g., maximum Feret diameter, equivalent circular perimeter diameter, and least bounding circle. Determination of particle sizes for microscopy analysis has, therefore, more freedom in selecting the parameter of interest. Another advantage of microscopy over other methods is the fact that the images of the particles being analyzed can be stored and examined manually. By far, the biggest challenge for dynamic microscopy analysis is the limited depth of field. The small field of view should be representative for a given lot and is prone to introduce underrepresented statistics, as only a small fraction of the passing flow is analyzed. According to Shekunov [182], by following ISO 14488, the minimum number of particles should typically be above 1,000,000 particles to achieve a maximum PSD error of $<1\%$. Furthermore, the limited depth of field also poses a challenge as particles out of focus is likely to be wrongly perceived.

5.4. Discrimination

As a result of diversity in theoretical background and technique, the selection of the appropriate online TSS monitoring technique depends on the characteristics of the different materials to be analyzed, such as physical form, particle size range, and particle concentration. Generally, meaningful particle size measurements must be derived from well described experiments, sample technique, and sample's properties and characteristics [171]. Most of the described methods in this section suffer from the fact that even as a PSD is obtained quickly and the number of particles is counted accurately, the highly sophisticated method for measuring the particle sizes is based on simple mathematical equations of calculation the equivalent diameter of a sphere and the existing shape influence are not taken into the equation [167]. Besides microscopy, which is based on direct observation, all other highlighted techniques in Section 5 are indirect methods based on different property of particles, except turbidimetry. For those indirect methods, the particle size is often obtained from characteristics of the sample that are well known and determined based on a calibration curve, assuming the particles to be perfectly spherical. These indirect methods work well in processes where the particles of interest are dominant. However, in processes where the sample is diverse and, to some extent, "unknown", the indirect methods are challenged by their property assumptions. Figure 18 presents what type of information different types of methods can provide.

As highlighted at the beginning of this section (Section 5), turbidity cannot bring any information about the particle size nor particle counts. However, knowing the change in TSS concentration by measuring the turbidity of the IW might be a useful support for measuring the particle sizes. The data information provided by indirect methods is more sensitive to particulate concentration changes than turbidimeters and thus offer additional information about process changes [178]. The challenge should be found in the highly sophisticated indirect methods for measuring the particle sizes are based on the equivalent diameter of a sphere, which bring little or no information about the what type of particles are present, and can even output particle size measurements incorrectly when the particles deviate extensively from being spherical. Another significant advantage of microscopy compared to other measurement techniques is the ability to discriminate particles captured by the equipment manually. The absence of manual justification of particle classification is a general disadvantage whenever particle sizes are quantified based on an indirect method.

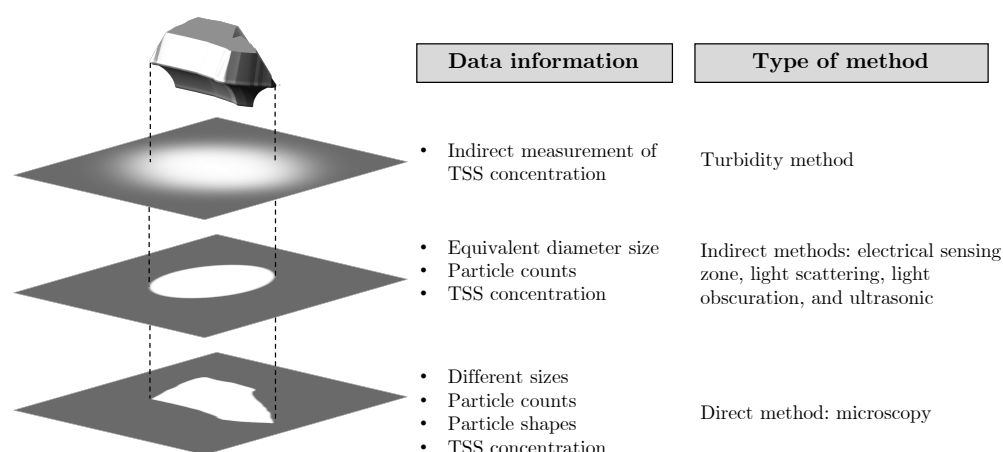


Figure 18. Illustration of data information available based on different type of particle analysis methods.

There exist several commercially available microscopy analyzers. Some are already installed as trials to measure oil droplets and solid particles sizes and their concentration in the oil and gas industry. The amount of different applications for each microscopy type of measurement is great. The assortment of microscopy monitors is selected based on diversity in their measurement design, connection, detections, and current presence in the oil and gas industry.

It can be challenging to assess each microscopy analyzer's strengths and limitations based on performance in different documentations. Therefore, the list is not based on performance in different publications, but only specifications provided by companies in their manuals, publications, and websites. The price and complexity of various microscopic monitors vary tremendously. Particle examination with microscopy is generally at the high-end of the market, compared to the other methods, i.e., turbidimeters, which only cost a fraction of microscopy analyzers [169]. In addition to being financially expensive to invest in a microscopy analyzer, the manufacturers offer services, such as courses, installation, and maintenance. Due to the offered services, there might be a general tendency for incomplete documentation and guidance of their software's potential, as it incentivizes the manufacturers to retain their documentation as confidential and enhance the demand of their offered services. According to Shand [194], manufacturers who do not offer a detailed description of the user manual can make the implementation process difficult, particularly if parts of the product are not defined or if users find discrepancies between the product and the user manual, and thereby have difficulties determining which one is the true statement [194]. Shand [194] further suggests that the user manual must be written as the same quality that would be expected at the quality of the product. The cost of poorly written user manuals for both the supplier and manufacturer can be high, but it is seldom calculated [194].

In Table 8, J.M. Canty InFlow and Jorin ViPA are selected based on the familiarity in the offshore oil and gas industry [195,196]: they are ATEX approved, have been in the business for several years, and have the knowledge of the challenges related to offshore installations. Thus, they can handle hazardous environments. Both monitors are similar in their design, where liquid flows through a flow cell while taking pictures from one side of the flow cell window and on the opposite side of the window a light source. The monitors then capture the oriented area of the objects perpendicular to the camera with a frame rate of ~30 Hz, respectively. Besides their software design and selection of different hardware, they basically use the same principles and can output more or less the same parameters of each object. For Jorin ViPA, it is up to the operator to determine the discrimination based on the different parameter ranges selected, which gives freedom and entrusts the operators to be specialists in their instrument to use it properly. That may sound positive, but with a lack of detailed description of the instrument software, the freedom to adjust every value can become a challenge to evaluate its influence on the outcome result. The J.M. Canty

InFlow uses neural networks/machine learning to classify different objects. That gives the operator the option to train the classifier to become more accurate without tuning every parameter manually to define a class. That increment of the human–computer interaction (HCI) feature should undoubtedly ease the classification process to classify each particle more correctly. Another benefit of the J.M. Canty InFlow compared to Jorin ViPA is the selection of having an automatic cleaning procedure for removing any fouling on the view cell.

Grundfos Bacmon and ParticleTech oCelloScope are very similar in their design by letting the sample through the flow cell. The sample is then captured and held still between the inlet and outlet while the scanning procedure is running. The scanning procedure is executed along the flow cell with a tilted camera, causing each particle to be recorded several times at different locations. By stacking the sliced image planes of the flow sample, it is possible to create 3D images of the present particles to overcome the limitation of only capturing the oriented area [197,198]. The shape information inadequacy of two-dimensional image analysis was already in the late 1980s described by Leschonski [167]:

“...two-dimensional image cannot yield information on the three-dimensional particle unless the particle is either rotated or cut into slices during analysis.”

or




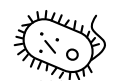

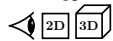
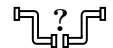
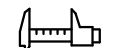
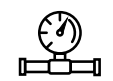
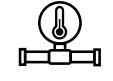
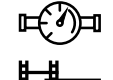



“...three-dimensional shape will at least demand information to be taken from three perpendicular planes.”

The Bacmon monitor is specifically developed to distinguish between bacteria and abiotic particles in drinking water. The classification is done by neural networks establishing a boundary between bacteria and abiotic particles in a 59-dimensional parameter space. Theirs developed library includes a prefix of different morphological shapes, such as rods, curved rods, and cocci, as well as various abiotic particle morphologies, e.g., clay [198]. Compared to Grundfos, ParticleTech has a broader application focus, such as crystallization, sand, and fermentation. However, it difficult to distinguish between both instruments as the available information about the ParticleTech analyzer system is limited. One promising solution presented by ParticleTech is how the manually defined particle classes can be represented by colors after the analysis, which is convenient for operators. Last, the two microscopy analyzers—SOPAT MM2 and Ma—from Table 8 are similar in their design. The reason for adding both to the list is simply to show that one manufacture can have several products that could be of interest. The same applies to the InFlow by J.M. Canty, which has multiple design selections to customize the unit for each customer’s need. The SOPAT microscopy analyzers are endoscopic devices that enable in-line installations in the process, assuming that the process has different sensor lock-gates installed. According to Panckow [199], SOPAT microscopy analyzers can automatically output the equivalent diameter and detect irregular shapes by analyzing the edges of expected particles. It should be possible to evaluate each particle manually by means of an integrated interface tool [199]. Their design as an endoscope is what differentiates them from other microscopy analyzers, like Jorin ViPA and J.M. Canty InFlow. It can be useful in processes where only spot checks are necessary at different locations, which require only one monitor, or in volumes where accurate on-line sampling is troublesome, like analyzing the homogeneity in a tank at different levels and locations. All five microscopy analyzers adequately cover the necessary TSS measurement criteria at an offshore IWT process, based on the evaluation in Section 3, to discriminate between different particles, as a minimum between bubbles, droplets, and solids. The authors highly recommend using identical microscopy analyzers in the entire process to reduce the uncertainty between different monitors [55].

The Jorin ViPA and the J.M. Canty InFlow monitors have the advantage of being familiar with the oil and gas industry. Though, J.M. Canty InFlow may satisfy the application mostly as they have an automatic cleaning procedure and strive to ease the classification process of discriminating different bubbles, droplets, and solids. An automatic cleaning procedure of the view cell is highly favored, if not a demand. HCI classification process

by J.M. Canty InFlow and ParticleTech's colorization of each particle class objects are software features that companies should strive to incorporate in their software design to ease operators' work. Furthermore, microscopy analyzers would draw the benefit of striving for measuring 3D images of particles, e.g., Bacmon and ParticleTech, to remove the limitation of only being the oriented area of particles in a 2D image that is measured. Thus, 3D images enhance the classification of each particle and increase accuracy. However, it should be noted that 3D image analysis introduces additional complexity. Suppose a sampling point for on-line monitor is considered to misrepresent the mainstream, or operators are discerning an undesired maldistribution at specific areas in the process. In that case, an alternative could be an in-line endoscope analyzer, e.g., SOPAT, to measure the TSS parameters at different levels in the process stream. The installment of in-line sensor lock-gates also benefits for measuring TSS parameters at locations where continuous online monitoring is not particularly necessary.

Table 8. A non-exhaustive list with a comparison of five different image analysis monitors' design and options available.

	Manufacturer Instrument Name	Jorin ViPA	J.M. Cauty InFlow	Grundfos Bacmon	ParticleTech oCelloScope	SOPAT MM2, Ma
Familiar with the oil and gas industry		✓	✓	✗	✗	(✓) *
Distinguish between solids, droplets, and bubbles		✓	✓	(✓)	(✓)	✓
Categorize different solid types		✓	✓	✓	✓	✓
Distinguish bacteria and abiotic particles		✗	✗	✓	✓	✗
Training classification (neural network, machine learning)		✗	✓	✓	✗	✗
View		2D	2D	3D	3D	2D
Connection		At-line/on-line	At-line/on-line/(in-line)	At-line/on-line	At-line	In-line
Measurement range [μm]		<150 **	0.7 – 480	0.6 < **	0.5 < and >2000	0.5 – 90, 1.5 – 280
Pressure range [Bar]		<120	<689	2 – 10	—	0.01 – 3, 0.01 – 320
Temperature range [°C]		<120	—	5 – 40	20 – 40 (operation temp.)	0 – 50
Flow velocity [m/s]		0.03 – 2.1 (0.05 – 4)L/min	0.25 – 2.74	Batch operation, 10 min cycle	Batch operation, 10 min cycle	—
Frame rate [Hz]		30	30	—	—	15
Cleaning procedure		Manually with flexible stick	Automatically vapor removal system	Flushed between each batch cycle for 1 min	Flushed between each batch	Automatically liquid cleaner (Ceramat Sensor Lock-Gate)
ATEX approved		✓	✓	✗	✗	✗, ✓

* Applied at a testing facility related to upstream oil-water separation process. However, to the authors knowledge it has not been installed at a fully integrated upstream separation process. ** Minimum or maximum measurement range is not explicitly defined.

6. Conclusions

Global oil production is still expected to increase in the next 30 years according to EIA. In the world's transition to becoming CO₂ neutral, developed countries have a responsibility not to force the emission of GHG outside their borders. The oil and gas industry can play a part in the transition by continually investing in the most innovative solutions that improve energy efficiency and researching new technologies that minimize GHG emissions. The importance of accurate online water quality measurements increase every year in the oil and gas industry to purify the produced water before discharge or reinjecting it into the reservoir. The water analysis and online measurement of TSS can assist in identifying and locating contamination in the process, and providing decision support for addition of chemicals or for process design changes. For online TSS monitors to be useful, the solution must be representatively sampled, and the sample must be withdrawn, analyzed, and interpreted correctly. Action mislead by inaccurate TSS measurements can cause more harm than not taking any action at all. Online measurement of TSS can be used for decision support, localization of possible contamination, and assist in confirming if past changes in water treatment have any effect on the water quality. Online measurement of TSS parameters can be used for advanced control to improve the treatment process. Even though the methods and designs of different TSS monitors reviewed in this paper are related to offshore IWT facilities, most of them are applicable to other domains such as other water treatment and biofuel facilities. The importance of water quality for maintaining long-term water injection of both produced water and seawater has been reviewed in detail in this paper. Maintaining a long-term water injection is usually related directly or indirectly to the water quality. However, the net present value of maintaining this high water quality should be justified against the net present value of other alternatives, e.g., periodic well-stimulation.

The majority of injectivity reductions are caused by a combination of different interlinked water quality problems. This paper analyzed several water quality effects that add to the TSS concentration, such as suspended solids, oil content from produced water reinjection, scales, corrosion disposal, and bacterial growth. A case study of measuring the TSS concentration of seawater from the Danish sector of the North Sea has been executed. The results from the case study of the seawater were evaluated in order to effectively quantify water quality through the process of an IWT facility. The results showed that the selected particle size analyzer should be able to measure within an overall TSS concentration from $>30.5 \text{ mg/L } (\mu + 2\sigma)$ to $\sim 0 \text{ mg/L}$ for this particular IWT facility.

Several on- or in-line techniques have been evaluated as candidates for measuring TSS parameters. Through a discrimination process, based on the results in several studies, this study recommends measuring different TSS parameters with a microscopy analyzer will bring the most promising results. Most techniques suffer from the fact that their estimation of particle sizes are based on the equivalent diameter of a sphere, and the shape influence is not taken into account. The last part of the paper outlined five different microscopy analyzers for measuring TSS. Each microscopy analyzer has been compared, and an evaluation of future design considerations of microscopy analyzers have been discussed. This study suggests that the development of TSS monitors should present shape analysis to a much greater extend to increase the accuracy of the TSS parameters and correlate the shape information to other physical particle properties to better classify each particle to its morphology.

Author Contributions: Validation, D.S.H. and M.V.B.; investigation, D.S.H.; resources, S.M.Ø.L.; data curation, S.M.Ø.L.; writing—original draft preparation, D.S.H.; writing—review, D.S.H.; editing D.S.H., M.V.B., S.M.Ø.L., and Z.Y.; supervision, Z.Y.; funding acquisition, Z.Y. All authors have read and agreed to the published version of the manuscript.

Funding: This research was funded by DHRCT projects: “Injection Water Quality and Control” (Proj-no.: 878040).

Data Availability Statement: The data presented in this study are available on request from the corresponding author.

Acknowledgments: The authors would like to thank the support from the DTU DHRTC and thank the colleagues: L. Hansen, and S. Jespersen from AAU, for many valuable discussions and support. A special thanks go to colleagues at Total Danmark A/S in Esbjerg for valuable support.

Conflicts of Interest: The authors declare no conflict of interest.

Abbreviations

The following abbreviations are used in this manuscript:

APB	acid-producing bacteria
API	American Petroleum Institute
ASTM	American Society for Testing and Materials
CDOM	colored dissolved organic matter
EIA	Energy Information Administration
EOR	enhanced oil recovery
EPS	extracellular polymeric substance
ESZ	electrical sensing zone
FFT	fast Fourier transform
GHG	greenhouse gases
H ₀	null-hypotheses
HCI	human-computer interaction
IEA	International Energy Agency
IOB	iron/manganese-oxidizing bacteria
IRB	iron-reducing bacteria
ISO	International Organization for Standardization
IW	injection water
IWT	injection water treatment
MIC	microbially influenced corrosion
MDB	metal-depositing bacteria
MRB	metal-reducing bacteria
NGS	next-generation sequencing
NRB	nitrate-reducing bacteria
NTU	nephelometric turbidity units
OECD	Organisation for Economic Co-operation and Development
OIP	oil in place
OSPAR	Oslo and Paris Convention
ppm	parts per million
PSD	particle size distribution
PW	produced water
PWRI	produced water reinjection
SRB	sulfate-reducing bacteria
SFB	slime-forming bacteria
SSC	suspended sediment concentration
TDS	total dissolved solids
TPES	Total primary energy supply
TSS	total suspended solids
UV	ultraviolet

References

1. EIA. *International Energy Outlook 2019*; Technical Report; U.S. Energy Information Administration: Washington, DC, USA, 2019.
2. IEA. *Energy Access Outlook 2017*; Technical Report; International Energy Agency: Paris, France, 2017.
3. EIA. *International Energy Outlook 2019: World Energy Projection System Plus*; U.S. Energy Information Administration: Washington, DC, USA, 2019.
4. SEI; IISD; ODI; Analytics Climate; CICERO; UNEP. *The Production Gap: The Discrepancy between Countries' Planned Fossil Fuel Production and Global Production Levels Consistent with Limiting Warming to 1.5 °C or 2 °C*; Technical Report; The Production Gap: Geneva, Switzerland, 2019.

5. IPIECA. *Meeting Energy Needs: The Unique Role of Oil and Gas*; Technical Report; The Global Oil and Gas Industry Association for Environmental and Social Issues: London, UK, 2014.
6. Capodaglio, A.G.; Callegari, A. Online Monitoring Technologies For Drinking Water Systems Security. In *Risk Management of Water Supply and Sanitation Systems*; NATO Science for Peace and Security Series C: Environmental Security; Hlavinec, P., Popovska, C., Marsalek, J., Mahrikova, I., Kukharchyk, T., Eds.; Springer: Dordrecht, The Netherlands, 2009; pp. 153–179. [\[CrossRef\]](#)
7. Blanchard, E. Oil in Water Monitoring is a Key to Production Separation. *Offshore* **2013**, *73*, 104–105.
8. Maxwell, S. Implications of Re-Injection of Produced Water on Microbially Influenced Corrosion (MIC) in Offshore Water Injection Systems. In *Proceedings of the CORROSION 2005*, Houston, TX, USA, 3–7 April 2005; p. 9.
9. OSPAR Commission. *List of Decisions, Recommendations and Other Agreements Applicable within the Framework of the OSPAR Convention—Update 2018*; Technical Report; OSPAR: London, UK, 2018.
10. Severin Hansen, D.; Jespersen, S.; Bram, M.V.; Yang, Z. Uncertainty Analysis of Fluorescence-Based Oil-In-Water Monitors for Oil and Gas Produced Water. *Sensors* **2020**, *20*, 36. [\[CrossRef\]](#) [\[PubMed\]](#)
11. Bavière, M. *Basic Concepts in Enhanced Oil Recovery Processes*, 1st ed.; Critical Reports on Applied Chemistry Volume 33; Elsevier: London, UK, 1991; pp. v–viii.
12. Hartmann, D.J.; Beaumont, E.A. Predicting Reservoir System Quality and Performance. In *Handbook of Petroleum Geology: Exploring for Oil and Gas Traps*, 1st ed.; Beaumont, E.A., Foster, N.H., Eds.; The American Association of Petroleum Geologists: Tulsa, OK, USA, 1999; Volume 3, Chapter 9, p. 154. [\[CrossRef\]](#)
13. Petroleum Council National; Enhanced Recovery Techniques; Committee on National Petroleum Council. *Enhanced Oil Recovery, EOR: An Analysis of the Potential for Enhanced Oil Recovery from Known Fields in the United States, 1976 to 2000*, 1st ed.; National Petroleum Council: Washington, DC, USA, 1976; p. 231.
14. Marle, C.M. Oil entrapment and mobilization. In *Basic Concepts in Enhanced Oil Recovery Processes*, 1st ed.; Bavière, M., Ed.; Elsevier: Essex, UK, 1991; Volume 33, Chapter 1, pp. 3–39.
15. British Petroleum. *BP Statistical Review of World Energy June 2017*; Technical Report; British Petroleum: London, UK, 2017.
16. Ostroff, A. Injection Water Problems Identified By Laboratory Analysis. In *Middle East Technical Conference and Exhibition*; Society of Petroleum Engineers: Manama, Bahrain, 1981; pp. 523–526. [\[CrossRef\]](#)
17. Carll, J.F. *The Geology of the Oil Regions of Warren, Venango, Clarion, and Butler Counties; Including Surveys of the Garland and Panama conglomerates in Warren and Crawford, and in Chautauqua Co., N. Y., Descriptions of Oil Well Rig and Tools, and a Discussion of th*, 1st ed.; Report of Progress; Harrisburg: Board of Commissioners for the Second Geological Survey: Washington, DC, USA, 1880; pp. 256–269.
18. Simmons, A.C. Recent Developments in Water Flooding in the Bradford District. In *Drilling and Production Practice*; American Petroleum Institute: Amarillo, TX, USA, 1938; pp. 260–266.
19. Cerini, W.F.; Battles, W.R.; Jones, P. Some Factors Influencing the Plugging Characteristics of an Oil-well Injection Water. *Trans. AIME* **1946**, *165*, 52–63. [\[CrossRef\]](#)
20. Babson, E.; Sherborne, J.; Jones, P. An Experimental Water-flood in a California Oil Field. *Trans. AIME* **1944**, *160*, 25–33. [\[CrossRef\]](#)
21. Ellenberger, A.R.; Holben, J.H. Flood Water Analyses and Interpretation. *J. Pet. Technol.* **1959**, *11*, 22–25. [\[CrossRef\]](#)
22. Watkins, J.W.; Willett, F.R., Jr.; Arthur, C.E. *Conditioning Water for Secondary-Recovery in Midcontinent Oil Fields*; Technical Report; Bureau of Mines: Bartlesville, OK, USA; Washington, DC, USA, 1952.
23. Safari, M. Effect of Different Water Injection Rate on Reservoir Performance: A Case Study of Azadegan Fractured Oil Reservoir. In *Proceedings of the International Conference of Oil, Gas, Petrochemical and Power Plant*, Tehran, Iran, 16 July 2012; Volume 1, p. 8.
24. Yu, K.; Li, K.; Li, Q.; Li, K.; Yang, F. A method to calculate reasonable water injection rate for M oilfield. *J. Pet. Explor. Prod. Technol.* **2017**, *7*, 1003–1010. [\[CrossRef\]](#)
25. Bansal, K.; Caudle, D. A New Approach for Injection Water Quality. In *Proceedings of the SPE Annual Technical Conference and Exhibition*, Washington, DC, USA, 4–7 October 1992; pp. 383–396. [\[CrossRef\]](#)
26. Patton, C.C. Water Quality Control and Its Importance in Waterflooding Operations. *J. Pet. Technol.* **1988**, *40*, 1123–1126. [\[CrossRef\]](#)
27. Yari, M.; Mansouri, H.; Esmaili, H.; Alavi, S.A. A Study of Microbial Influenced Corrosion in Oil and Gas Industry. In *International Conference of Oil, Gas, Petrochemical and Power Plant*; Civilica: Tehran, Iran, 2012; Volume 1, p. 11. [\[CrossRef\]](#)
28. Rochon, J.; Creusot, M.; Rivet, P.; Roque, C.; Renard, M. Water Quality for Water Injection Wells. In *SPE Formation Damage Control Symposium*; Society of Petroleum Engineers, Society of Petroleum Engineers: Lafayette, LA, USA, 1996; pp. 489–503. [\[CrossRef\]](#)
29. Mitchell, R.W. The Forties Field Sea Water Injection System. *J. Pet. Technol.* **1978**, *30*, 877–884. [\[CrossRef\]](#)
30. Mitchell, R.W.; Finch, E.M. Water Quality Aspects of North Sea Injection Water. *J. Pet. Technol.* **1981**, *33*, 1141–1152. [\[CrossRef\]](#)
31. Prandle, D.; Hydes, D.J.; Jarvis, J.; McManus, J. The Seasonal Cycles of Temperature, Salinity, Nutrients and Suspended Sediment in the Southern North Sea in 1988 and 1989. *Estuarine Coast. Shelf Sci.* **1997**, *45*, 669–680. [\[CrossRef\]](#)
32. Eisma, D.; Cadee, G.C.; Laane, R.W.P.M. Supply of Suspended Matter and Particulate and Dissolved Organic Carbon from the Rhine to the Coastal North Sea. *Transp. Carbon Miner. Major World Rivers* **1982**, *52*, 483–506.
33. Aguirre-Gómez, R. Detection of total suspended sediments in the North Sea using AVHRR and ship data. *Int. J. Remote. Sens.* **2000**, *21*, 1583–1596. [\[CrossRef\]](#)

34. Krumbein, W.C. Application of Logarithmic Moments to Size Frequency Distributions of Sediments. *J. Sediment. Res.* **1936**, *6*, 35–47. [\[CrossRef\]](#)
35. Udden, J.A. *The Mechanical Composition of Wind Deposits*, 1st ed.; Number 1; Augustana College and Theological Seminary: Rock Island, IL, USA, 1898; p. 69.
36. Wentworth, C.K. A Scale of Grade and Class Terms for Clastic Sediments. *J. Geol.* **1922**, *30*, 377–392. [\[CrossRef\]](#)
37. Blott, S.J.; Pye, K. Particle Size Scales and Classification of Sediment Types Based on Particle Size Distributions: Review and Recommended Procedures. *Sedimentology* **2012**, *59*, 2071–2096. [\[CrossRef\]](#)
38. Barkman, J.; Davidson, D. Measuring Water Quality and Predicting Well Impairment. *J. Pet. Technol.* **1972**, *24*, 865–873. [\[CrossRef\]](#)
39. Patton, C.C. Injection-Water Quality. *J. Pet. Technol.* **1990**, *42*, 1238–1240. [\[CrossRef\]](#)
40. Bennion, D.; Bennion, D.; Thomas, F.; Bietz, R. Injection Water Quality—A Key Factor to Successful Waterflooding. In Proceedings of the 45th Annual Technical Meeting, Calgary, AB, Canada, 12–15 June 1994; Volume 37, pp. 53–62. [\[CrossRef\]](#)
41. Bennion, D.; Thomas, F.; Imer, D.; Ma, T.; Schulmeister, B. Water Quality Considerations Resulting in the Impaired Injectivity of Water Injection and Disposal Wells. *J. Can. Pet. Technol.* **2001**, *40*, 54–61. [\[CrossRef\]](#)
42. Ogden, B.L. Water Technology: Understanding, Interpreting and Utilizing Water Analysis Data. In *Southwestern Petroleum Short Course Conference 2008*; Southwestern Petroleum Short Course: Lubbock, TX, USA, 2008; p. 12.
43. Donham, J. Offshore Water Injection System: Problems and Solutions. In Proceedings of the Offshore Technology Conference, Houston, TX, USA, 6–9 May 1991; pp. 53–57. [\[CrossRef\]](#)
44. Bader, M. Seawater versus produced water in oil-fields water injection operations. *Desalination* **2007**, *208*, 159–168. [\[CrossRef\]](#)
45. Gao, C. Factors affecting particle retention in porous media. *Emir. J. Eng. Res.* **2007**, *12*, 7.
46. Nielsen, B.L.; Nygaard, E.; Reffstrup, J.; Ter-Borch, N. *Bjergarters Reservoirregenskaber*; GEUS: Copenhagen, Denmark, 2019.
47. Abramovitz, T. Geophysical imaging of porosity variations in the Danish North Sea chalk. *Geol. Surv. Den. Greenl. Bull.* **2008**, *15*, 17–20. [\[CrossRef\]](#)
48. Jørgensen, L.N.; Andersen, P.M. Integrated Study of the Kraka Field. In *Offshore Europe*; Society of Petroleum Engineers: Aberdeen, China, 1991; pp. 461–474. [\[CrossRef\]](#)
49. Hardman, R.F.P. Chalk reservoirs of the North Sea. *Bull. Geol. Soc. Den.* **1982**, *30*, 119–137.
50. Torsaeter, O. An Experimental Study of Water Imbibition in Chalk From the Ekofisk Field. In *SPE Enhanced Oil Recovery Symposium*; Society of Petroleum Engineers: Tulsa, OK, USA, 1984; Volume 2, pp. 93–104. [\[CrossRef\]](#)
51. Shutong, P.; Sharma, M. A Model for Predicting Injectivity Decline in Water-Injection Wells. *SPE Form. Eval.* **1997**, *12*, 194–201. [\[CrossRef\]](#)
52. Eylander, J. Suspended Solids Specifications for Water Injection From Coreflood Tests. *SPE Reserv. Eng.* **1988**, *3*, 1287–1294. [\[CrossRef\]](#)
53. Hansen, D.S.; Jespersen, S.; Bram, M.V.; Yang, Z. Human Machine Interface Prototyping and Application for Advanced Control of Offshore Topside Separation Processes. In Proceedings of the IECON 2018—44th Annual Conference of the IEEE Industrial Electronics Society, Washington, DC, USA, 21–23 October 2018; pp. 2341–2347. [\[CrossRef\]](#)
54. Hansen, D.S.; Bram, M.V.; Yang, Z. Efficiency investigation of an offshore deoiling hydrocyclone using real-time fluorescence- and microscopy-based monitors. In Proceedings of the 2017 IEEE Conference on Control Technology and Applications (CCTA), Mauna Lani, HI, USA, 27–30 August 2017; pp. 1104–1109. [\[CrossRef\]](#)
55. Yang, M. Measurement of Oil in Produced Water. In *Produced Water*, 1st ed.; Lee, K., Neff, J., Eds.; Springer: New York, NY, USA, 2011; Chapter 2, pp. 57–88. [\[CrossRef\]](#)
56. Miløstyrelsen. *Generel Tilladelse for Total E&P Danmark A/S (TOTAL) Til Anvendelse, Udledning OG Anden Bortskaffelse af Stoffer OG Materialer, Herunder Olie OG Kemikalier i Produktions- OG Injektionsvand Fra Produktionsenhederne Halfdan, Dan, Tyra og Gorm for perioden 1 January 2019–31 December 2020*; Technical Report; Total E&P Danmark A/S: Copenhagen, Denmark, 2018.
57. Danish Energy Agency. *Production*; Technical Report; Danish Energy Agency: Esbjerg, Denmark, 2016.
58. Hansen, D.; Bram, M.; Durdevic, P.; Jespersen, S.; Yang, Z. Efficiency evaluation of offshore deoiling applications utilizing real-time oil-in-water monitors. In Proceedings of the Oceans 2017—Anchorage, Anchorage, AK, USA, 18–21 September 2017; p. 6.
59. Danish Energy Agency. *Yearly Production, Injection, Flare, Fuel and Export in SI Units 1972–2019*; The Danish Energy Agency: Copenhagen, Denmark, 2020.
60. OSPAR Commission. *Produced Water Discharges from Offshore Oil and Gas Installations 2007–2012*; OSPAR Commission: London, UK, 2014.
61. Miløstyrelsen. *Generel Tilladelse for Maersk Olie og Gas A/S (Maersk Olie) til Anvendelse, Udledning og Anden Bortskaffelse af Stoffer og Materialer, Herunder olie og Kemikalier i Produktions- og Injektionsvand fra Produktionsenhederne Halfdan, Dan, Tyra og Gorm for Perioden 1 January 2017–31 December 2018*; Technical Report; Mærsk Olie og Gas A/S: Copenhagen, Denmark, 2016.
62. OSPAR Commission. *OSPAR Report on Discharges, Spills and Emissions from Offshore Oil and Gas Installations in 2014*; Technical Report; OSPAR: London, UK, 2016.
63. Kokal, S.; Al-Dawood, N.; Fontanilla, J.; Al-Ghamdi, A.; Nasr-El-Din, H.; Al-Rufaie, Y. Productivity Decline in Oil Wells Related to Asphaltene Precipitation and Emulsion Blocks. *SPE Prod. Facil.* **2003**, *18*, 247–256. [\[CrossRef\]](#)

64. Baird, R.B.; Eaton, A.D.; Rice, E.W. *Standard Methods for the Examination of Water and Wastewater*, 23rd ed.; American Public Health Association, American Water Works Association, and Water Environment Federation: Washington, DC, USA, 2017; Chapter 2, pp. 66–82.
65. Allhands, M.N. *The Efficient Removal of Organic and Inorganic Suspended Solids—Old Problem, New Technology*; Water Online News: Horsham, PA, USA, 2016.
66. Kennicutt, M.C. Water Quality of the Gulf of Mexico. In *Habitats and Biota of the Gulf of Mexico: Before the Deepwater Horizon Oil Spill*, 1st ed.; Ward, C.H., Ed.; Springer: New York, NY, USA, 2017; Volume 1, Chapter 2, pp. 55–164. [\[CrossRef\]](#)
67. Boyd, C.E. Dissolved Solids. In *Water Quality*, 2nd ed.; Boyd, C.E., Ed.; Springer: Cham, Switzerland, 2015; Chapter 4, pp. 71–100. [\[CrossRef\]](#)
68. Nasr-El-Din, H.; Al-Taq, A. Water Quality Requirements and Restoring the Injectivity of Waste Water Disposal Wells. In *SPE Formation Damage Control Conference*; Society of Petroleum Engineers: Lafayette, LA, USA, 1998; pp. 565–573. [\[CrossRef\]](#)
69. Zheng, J.; Chen, B.; Thanyamanta, W.; Hawboldt, K.; Zhang, B.; Liu, B. Offshore produced water management: A review of current practice and challenges in harsh/Arctic environments. *Mar. Pollut. Bull.* **2016**, *104*, 7–19. [\[CrossRef\]](#) [\[PubMed\]](#)
70. Coleman, J.; McLelland, W. Produced Water Re-Injection; How Clean is Clean? In *SPE Formation Damage Control Symposium*; Society of Petroleum Engineers: Lafayette, LA, USA, 1994; p. 5. [\[CrossRef\]](#)
71. Jepsen, K.; Bram, M.; Pedersen, S.; Yang, Z. Membrane Fouling for Produced Water Treatment: A Review Study From a Process Control Perspective. *Water* **2018**, *10*, 847. [\[CrossRef\]](#)
72. Owen, G.; Bandi, M.; Howell, J.A.; Churchouse, S.J. Economic assessment of membrane processes for water and waste water treatment. *J. Membr. Sci.* **1995**, *102*, 77–91. [\[CrossRef\]](#)
73. van Oort, E.; van Velzen, J.; Leerlooijer, K. Impairment by Suspended Solids Invasion: Testing and Prediction. *SPE Prod. Facil.* **1993**, *8*, 178–184. [\[CrossRef\]](#)
74. Kwon, D.Y.; Vigneswaran, S.; Fane, A.G.; Aim, R.B. Experimental determination of critical flux in cross-flow microfiltration. *Sep. Purif. Technol.* **2000**, *19*, 169–181. [\[CrossRef\]](#)
75. Pautz, J.; Crocker, M.; Walton, C. Relating Water Quality and Formation Permeability to Loss of Injectivity. In *SPE Production Operations Symposium*; Society of Petroleum Engineers: Oklahoma City, OK, USA, 1989; pp. 565–576. [\[CrossRef\]](#)
76. Abrams, A. Mud Design To Minimize Rock Impairment Due To Particle Invasion. *J. Pet. Technol.* **1977**, *29*, 586–592. [\[CrossRef\]](#)
77. Wang, S.; Civan, F. Preventing Asphaltene Deposition in Oil Reservoirs by Early Water Injection. In *SPE Production Operations Symposium*; Society of Petroleum Engineers: Oklahoma City, OK, USA, 2005; p. 14. [\[CrossRef\]](#)
78. Permadi, A.K.; Naser, M.A.; Mucharam, L.; Rachmat, S.; Kishita, A. Formation Damage and Permeability Impairment Associated with Chemical and Thermal Treatments: Future Challenges in EOR Applications. In *The Contribution of Geosciences to Human Security*, 1st ed.; Kyoto University GCOE Program of HSE; Institut Teknologi Bandung, Kyoto University: Berlin, Germany, 2012; Chapter 7, pp. 103–126.
79. Khilar, K.C.; Vaidya, R.; Fogler, H. Colloidally-induced fines release in porous media. *J. Pet. Sci. Eng.* **1990**, *4*, 213–221. [\[CrossRef\]](#)
80. Bazin, B.; Esperanza, S.; Le Thiez, P. Control of Formation Damage by Modeling Water/Rock Interaction. In *SPE Formation Damage Control Symposium*; Society of Petroleum Engineers: Lafayette, LA, USA, 1994; pp. 249–258. [\[CrossRef\]](#)
81. Shrestha, R.A.; Zhang, A.P.; Mateus, E.P.; Ribeiro, A.B.; Pamukcu, S. Electrokinetically Enabled De-swelling of Clay. In *Electrokinetics Across Disciplines and Continents*; Ribeiro, A.B., Mateus, E.P., Couto, N., Eds.; Springer: Cham, Switzerland, 2016; Chapter 3, pp. 43–56. [\[CrossRef\]](#)
82. Merdhah, A.B.B.M. The Study of Scale Formation in Oil Reservoir during Water Injection at High-Barium and High-Salinity Formation Water. Ph.D. Thesis, Universiti Teknologi Malaysia, Skudai, Malaysia, 2008.
83. Amiri, M.; Moghadasi, J. Prediction the Amount of Barium Sulfate Scale Formation in Siri Oilfield using OLI ScaleChem Software. *Asian J. Sci. Res.* **2010**, *3*, 230–239. [\[CrossRef\]](#)
84. Amiri, M.; Moghadasi, J.; Jamialahmadi, M. Prediction of Iron Carbonate Scale Formation in Iranian Oilfields at Different Mixing Ratio of Injection Water with Formation Water. *Energy Sources Part Recover. Util. Environ. Eff.* **2013**, *35*, 1256–1265. [\[CrossRef\]](#)
85. Merdhah, A.B.B.; Yassin, A.A.M. Calcium and Strontium Sulfate Scale Formation Due to Incompatible Water. In *Proceedings of the International Graduate Conference on Engineering and Science 2008*, Johor, Malaysia, 23–24 December 2008; p. 9.
86. Collins, I.R.; Jordan, M.M. Occurrence, Prediction, and Prevention of Zinc Sulfide Scale Within Gulf Coast and North Sea High-Temperature and High-Salinity Fields. *SPE Prod. Facil.* **2003**, *18*, 200–209. [\[CrossRef\]](#)
87. Chester, R. Dissolved gases in sea water. In *Marine Geochemistry*, 1st ed.; Chester, R., Ed.; Springer: Dordrecht, The Netherlands, 1990; Chapter 8, pp. 233–271. [\[CrossRef\]](#)
88. Brondel, D.; Montrouge, F.; Edwards, R.; Hayman, A.; Hill, D.; Mehta, S.; Semerad, T. Corrosion in the Oil Industry. *Oilfield Rev.* **1994**, *6*, 4–18.
89. Ruschau, G.R.; Al-Anezi, A.M. Appendix S—Oil and Gas Exploration and Production. In *Corrosion Cost and Preventive Strategies in the United States*; Number FHWA-RD-01-156; Federal Highway Administration: McLean, VA, USA, 2001; Chapter Appendix S, p. 14.
90. Popoola, L.; Grema, A.; Latinwo, G.; Gutti, B.; Balogun, A. Corrosion problems during oil and gas production and its mitigation. *Int. J. Ind. Chem.* **2013**, *4*, 15. [\[CrossRef\]](#)
91. Koteeswaran, M. CO₂ and H₂S Corrosion in Oil Pipelines. Ph.D. Thesis, University of Stavanger, Stavanger, Norway, 2010.

92. Heidersbach, R. Corrosion in Oil and Gas Production. In *Microbiologically Influenced Corrosion in the Upstream Oil and Gas Industry*, 1st ed.; Skovhus, T.L., Enning, D., Lee, J.S., Eds.; CRC Press: Boca Raton, FL, USA, 2017; Chapter 1, pp. 3–34. [\[CrossRef\]](#)
93. Diaz, E.F.; Gonzalez-Rodriguez, J.G.; Martinez-Villafañe, A.; Gaona-Tiburcio, C. H₂S corrosion inhibition of an ultra high strength pipeline by carboxyethyl-imidazoline. *J. Appl. Electrochem.* **2010**, *40*, 1633–1640. [\[CrossRef\]](#)
94. Stansbury, E.E.; Buchanan, R.A. *Fundamentals of Electrochemical Corrosion*, 1st ed.; ASM International: Materials Park, OH, USA, 2000; p. 487.
95. Norsworthy, R. Understanding corrosion in underground pipelines: basic principles. In *Underground Pipeline Corrosion*, 1st ed.; Woodhead Publishing Series in Metals and Surface Engineering; Orazem, M.E., Ed.; Woodhead Publishing: Cambridge, UK, 2014; Chapter 1, pp. 3–34. [\[CrossRef\]](#)
96. Jomdecha, C.; Prateepasen, A.; Kaewtrakulpong, P. Study on source location using an acoustic emission system for various corrosion types. *NDT & E Int.* **2007**, *40*, 584–593. [\[CrossRef\]](#)
97. Landolt, D. Corrosion and Surface Treatment. In *Electrochemistry*; Feliu-Martinez, J.M., Paya, V.C., Eds.; EOLSS Publishers: Oxford, UK, 2009; Chapter 6, pp. 240–271.
98. American Water Works Association. Chemistry of Corrosion. In *M27—External Corrosion Control for Infrastructure Sustainability*, 3rd ed.; De Nileon, G.P., Gray, M.R., Armstrong, C., Beach, M., Eds.; Manual of Water Supply Practices, American Water Works Association: Denver, CO, USA, 2014; Chapter 2, pp. 7–24.
99. Byars, H.; Gallop, B. Injection Water + Oxygen = Corrosion and/or Well Plugging Solids. In *SPE Symposium on Handling of Oilfield Water*; Society of Petroleum Engineers: Los Angeles, CA, USA, 1972; pp. 96–102. [\[CrossRef\]](#)
100. Durdevic, P.; Raju, C.S.; Yang, Z. Potential for Real-Time Monitoring and Control of Dissolved Oxygen in the Injection Water Treatment Process. *IFAC PapersOnLine* **2018**, *51*, 170–177. [\[CrossRef\]](#)
101. Zardyneshad, S. *Consider Key Factors in Pipeline Wall Thickness Calculation and Selection*; Gas Process. & LNG: Louis, MO, USA, 2015.
102. Beavers, J.A.; Thompson, N.G. External corrosion of oil and natural gas pipelines. In *ASM handbook Volume 13C: Corrosion: Environments and Industries*, 1st ed.; ASM Handbook; Cramer, S.D., Bernard, S., Covino, J., Eds.; ASM International: Materials Park, OH, USA, 2006; Chapter 100, pp. 1015–1025. [\[CrossRef\]](#)
103. Shirazi, S.A.; McLaury, B.S.; Shadley, J.R.; Roberts, K.P.; Rybicki, E.F.; Rincon, H.E.; Hassani, S.; Al-Mutahar, F.M.; Al-Aithan, G.H. Erosion–Corrosion in Oil and Gas Pipelines. In *Oil and Gas Pipelines: Integrity and Safety Handbook*, 1st ed.; Revie, R.W., Ed.; John Wiley & Sons, Inc.: Hoboken, NJ, USA, 2015; Chapter 28, pp. 399–422. [\[CrossRef\]](#)
104. Sastri, V.S. Corrosion Causes. In *Challenges in Corrosion: Costs, Causes, Consequences, and Control*, 1st ed.; Revie, R.W., Ed.; Wiley Series in Corrosion; John Wiley & Sons: Hoboken, NJ, USA, 2015; Chapter 3, pp. 127–204. [\[CrossRef\]](#)
105. Farshad, F.F.; Choate, L.C.; Winters, R.H.; Garber, J.D. *Pipeline Optimization—A Surface Roughness Approach*; Technical Report; University of Louisiana: Lafayette, LA, USA, 2017.
106. Skovhus, T.L.; Enning, D.; Lee, J.S. *Microbiologically Influenced Corrosion in the Upstream Oil and Gas Industry*, 1st ed.; CRC Press: Boca Raton, FL, USA, 2017; pp. v–xxvi. [\[CrossRef\]](#)
107. Ren, H.; Xiong, S.; Gao, G.; Song, Y.; Cao, G.; Zhao, L.; Zhang, X. Bacteria in the injection water differently impacts the bacterial communities of production wells in high-temperature petroleum reservoirs. *Front. Microbiol.* **2015**, *6*, 8. [\[CrossRef\]](#)
108. Ismail, W.A.; Van Hamme, J.D.; Kilbane, J.J.; Gu, J.D. Editorial: Petroleum Microbial Biotechnology: Challenges and Prospects. *Front. Microbiol.* **2017**, *8*, 4. [\[CrossRef\]](#) [\[PubMed\]](#)
109. Bouchard, R.P. *Is a Virus a Living Creature?* Medium: San Francisco, CA, USA, 2017.
110. Wang, I.; Burckhardt, C.J.; Yakimovich, A.; Greber, U.F. Imaging, Tracking and Computational Analyses of Virus Entry and Egress with the Cytoskeleton. *Viruses* **2018**, *10*, 29. [\[CrossRef\]](#)
111. Cole, L.A. Evolutionary History of Planet Earth. In *Biology of Life: Biochemistry, Physiology and Philosophy*, 1st ed.; Tenney, S., Ed.; Academic Press: Cambridge, MA, USA, 2016; Chapter 6, pp. 37–43. [\[CrossRef\]](#)
112. Schloss, P.D.; Handelsman, J. Status of the Microbial Census. *Microbiol. Mol. Biol. Rev.* **2004**, *68*, 686–691. [\[CrossRef\]](#) [\[PubMed\]](#)
113. Whitman, W.B.; Coleman, D.C.; Wiebe, W.J. Prokaryotes: the unseen majority. *Proc. Natl. Acad. Sci. USA* **1998**, *95*, 6578–6583. [\[CrossRef\]](#) [\[PubMed\]](#)
114. Baron, E.J. Classification. In *Medical Microbiology*, 4th ed.; Baron, S., Ed.; University of Texas Medical Branch: Galveston, TX, USA, 1996; Chapter 3.
115. Gillespie, S.H.; Bamford, K.B. Structure and Classification of Bacteria. In *Medical Microbiology and Infection at a Glance*, 4th ed.; Wiley-Blackwell: Hoboken, NJ, USA, 2012; Chapter 1, pp. 8–9.
116. Barnes-Svarney, P.; Svarney, T.E. *The Handy Biology Answer Book*, 2nd ed.; Visible Ink Press: Canton, MI, USA, 2015; pp. 1–496.
117. Barer, M.R. Bacterial growth, physiology and death. In *Medical Microbiology: A Guide to Microbial Infections: Pathogenesis, Immunity, Laboratory Diagnosis and Control*, 18th ed.; Greenwood, D., Barer, M.R., Slack, R.C.B., Irving, W.L., Eds.; Churchill Livingstone: London, UK, 2012; Chapter 4, pp. 39–53. [\[CrossRef\]](#)
118. Beech, I.; Flemming, H.C.; Mollica, A.; Scotto, V. *Simple Methods for the Investigation of the Role of Biofilms in Corrosion*; Technical Report; European Commission Federation of Corrosion: Stockholm, Sweden, 2000.
119. MacLeod, R.A. The Question of the Existence of Specific Marine Bacteria. *Bacteriol. Rev.* **1965**, *29*, 9–24. [\[CrossRef\]](#)
120. Little, B.; Wagner, P.; Mansfeld, F. An Overview of Microbiologically Influenced Corrosion. *Electrochim. Acta* **1992**, *37*, 2185–2194. [\[CrossRef\]](#)

121. Little, B.J.; Lee, J.S. *Microbiologically Influenced Corrosion*, 1st ed.; John Wiley & Sons, Inc.: Hoboken, NJ, USA, 2007; p. 280. [\[CrossRef\]](#)
122. Heitz, E.; Flemming, H.C.; Sand, W. *Microbially Influenced Corrosion of Materials: Scientific and Engineering Aspects*, 1st ed.; Springer: Berlin/Heidelberg, Germany, 1996; p. 475.
123. Fischer, D.; Canalizo-Hernandez, M.; Kumar, A. Effects of Reservoir Souring on Materials Performance. In *Microbiologically Influenced Corrosion in the Upstream Oil and Gas Industry*, 1st ed.; Skovhus, T.L., Enning, D., Lee, J.S., Eds.; CRC Press: Boca Raton, FL, USA, 2017; Chapter 6, pp. 111–137. [\[CrossRef\]](#)
124. Mittelman, M.W. Bacterial Biofilms and Biofouling: Translational Research in Marine Biotechnology. In *Opportunities for Environmental Applications of Marine Biotechnology*; Vaupel, S., Ed.; National Academies Press: Washington, DC, USA, 2000; Chapter 2, pp. 3–7. [\[CrossRef\]](#)
125. Komlenic, R. Rethinking the causes of membrane biofouling. *Filtr. Sep.* **2010**, *47*, 26–28. [\[CrossRef\]](#)
126. Donlan, R.M. Biofilms: Microbial Life on Surfaces. *Emerg. Infect. Dis.* **2002**, *8*, 881–890. [\[CrossRef\]](#) [\[PubMed\]](#)
127. Vasudevan, R. Biofilms: Microbial Cities of Scientific Significance. *J. Microbiol. Exp.* **2014**, *1*, 1–16. [\[CrossRef\]](#)
128. Nguyen, T.; Roddick, F.; Fan, L. Biofouling of Water Treatment Membranes: A Review of the Underlying Causes, Monitoring Techniques and Control Measures. *Membranes* **2012**, *2*, 804–840. [\[CrossRef\]](#) [\[PubMed\]](#)
129. Sauer, K.; Camper, A.K.; Ehrlich, G.D.; Costerton, J.W.; Davies, D.G. *Pseudomonas aeruginosa* displays multiple phenotypes during development as a biofilm. *J. Bacteriol.* **2002**, *184*, 1140–1154. [\[CrossRef\]](#) [\[PubMed\]](#)
130. Macià, M.D.; Rojo-Molinero, E.; Oliver, A. Antimicrobial susceptibility testing in biofilm-growing bacteria. *Clin. Microbiol. Infect. Off. Publ. Eur. Soc. Clin. Microbiol. Infect. Dis.* **2014**, *20*, 981–990. [\[CrossRef\]](#) [\[PubMed\]](#)
131. Mah, T.F.C.; O'Toole, G.A. Mechanisms of biofilm resistance to antimicrobial agents. *Trends Microbiol.* **2001**, *9*, 34–39. [\[CrossRef\]](#)
132. Hall-Stoodley, L.; Costerton, J.W.; Stoodley, P. Bacterial biofilms: from the Natural environment to infectious diseases. *Nat. Rev. Microbiol.* **2004**, *2*, 95–108. [\[CrossRef\]](#)
133. Tidwell, T.J.; Keasler, V.; Paula, R.D. How Production Chemicals Can Influence Microbial Susceptibility to Biocides and Impact Mitigation Strategies. In *Microbiologically Influenced Corrosion in the Upstream Oil and Gas Industry*, 1st ed.; Skovhus, T.L., Enning, D., Lee, J.S., Eds.; CRC Press: Boca Raton, FL, USA, 2017; Chapter 19, pp. 379–392. [\[CrossRef\]](#)
134. Little, B.; Lee, J.; Ray, R. *New Developments in Mitigation of Microbiologically Influenced Corrosion*; Technical Report; Naval Research Laboratory Oceanography Division Stennis Space Center: Fort Belvoir, VA, USA, 2007.
135. Turkiewicz, A.; Brzeszcz, J.; Kapusta, P. The application of biocides in the oil and gas industry. *Nafta-Gaz* **2013**, *69*, 103–111. [\[CrossRef\]](#)
136. Laura Machuca Suarez. Microbiologically Induced Corrosion Associated with the Wet Storage of Subsea Pipelines (Wet Parking). In *Microbiologically Influenced Corrosion in the Upstream Oil and Gas Industry*, 1st ed.; Skovhus, T.L., Enning, D., Lee, J.S., Eds.; CRC Press: Boca Raton, FL, USA, 2017; Chapter 18, pp. 361–378. [\[CrossRef\]](#)
137. Javaherdashti, R. *Microbiologically Influenced Corrosion*, 2nd ed.; Engineering Materials and Processes; Springer: London, UK, 2008; p. 216. [\[CrossRef\]](#)
138. Sandbeck, K.; Hitzman, D. Biocompetitive Exclusion Technology: A Field System to Control Reservoir Souring and Increasing Production. In Proceedings of the Fifth International Conference on Microbial Enhanced Oil Recovery and Related Biotechnology for Solving Environment Problems, Dallas, TX, USA, 11–14 September 1995; pp. 311–319.
139. Schwermer, C.U.; Lavik, G.; Abed, R.M.M.; Dunsmore, B.; Ferdelman, T.G.; Stoodley, P.; Gieseke, A.; de Beer, D. Impact of Nitrate on the Structure and Function of Bacterial Biofilm Communities in Pipelines Used for Injection of Seawater into Oil Fields. *Appl. Environ. Microbiol.* **2008**, *74*, 2841–2851. [\[CrossRef\]](#)
140. Hubert, C.; Voordouw, G.; Arensdorf, J.; Jenneman, G.E. Control of souring through a novel class of bacteria that oxidize sulfide as well as oil organics with nitrate. In Proceedings of the CORROSION/2006, NACE International, San Diego, CA, USA, 12–16 March 2006; p. 10.
141. Xu, D. Microbiologically Influenced Corrosion (MIC) Mechanisms and Mitigation. Ph.D. Thesis, Ohio University, Athens, OH, USA, 2013.
142. Jones, S.E.; Lennon, J.T. Dormancy contributes to the maintenance of microbial diversity. *Proc. Natl. Acad. Sci. USA* **2010**, *107*, 5881–5886. [\[CrossRef\]](#)
143. Lewis, K. Persister cells, dormancy and infectious disease. *Nat. Rev. Microbiol.* **2007**, *5*, 48–56. [\[CrossRef\]](#)
144. El-Baky, R. The Future Challenges Facing Antimicrobial Therapy: Resistance and Persistence. *Am. J. Microbiol. Res.* **2016**, *4*, 15. [\[CrossRef\]](#)
145. Stewart, E.J. Growing Unculturable Bacteria. *J. Bacteriol.* **2012**, *194*, 4151–4160. [\[CrossRef\]](#)
146. Hu, A. Investigation of Sulfate-Reducing Bacteria Growth Behavior for the Mitigation of Microbiologically Influenced Corrosion (MIC). Ph.D. Thesis, Ohio University, Athens, OH, USA, 2004.
147. Klai, N.; Yan, S.; Tyagi, R.D.; Surampalli, R.Y. EPS producing microorganisms from municipal wastewater activated sludge. *J. Pet. Environ. Biotechnol.* **2016**, *7*, 13. [\[CrossRef\]](#)
148. Raulio, M. Ultrastructure of Biofilms Formed by Bacteria From Industrial Processes. Ph.D. Thesis, University of Helsinki, Helsinki, Finland, 2010.
149. Natarajan, K. Biofouling and Microbially Influenced Corrosion of Stainless Steels. *Adv. Mater. Res.* **2013**, *794*, 539–551. [\[CrossRef\]](#)

150. Borenstein, S.W. Microbiology. In *Microbiologically Influenced Corrosion Handbook*, 1st ed.; Woodhead Publishing: Cambridge, UK, 1994; Chapter 2, pp. 8–49. [\[CrossRef\]](#)
151. Coetser, S.E.; Cloete, T.E. Biofouling and Biocorrosion in Industrial Water Systems. *Crit. Rev. Microbiol.* **2005**, *31*, 213–232. [\[CrossRef\]](#) [\[PubMed\]](#)
152. Okabe, S.; Jones, W.L.; Lee, W.; Characklis, W.G. Anaerobic SRB Biofilms in Industrial Waters Systems: A process Analysis. In *Biofouling and Biocorrosion in Industrial Water Systems*, 1st ed.; Geesey, G.G., Lewandowski, Z., Flemming, H.C., Eds.; CRC Press: Boca Raton, FL, USA, 1994; Chapter 12, pp. 189–204.
153. Sharma, M.; Voordouw, G. MIC Detection and Assessment A Holistic Approach. In *Microbiologically Influenced Corrosion in the Upstream Oil and Gas Industry*, 1st ed.; Skovhus, T.L., Enning, D., Lee, J.S., Eds.; CRC Press: Boca Raton, FL, USA, 2017; Chapter 9, pp. 177–212. [\[CrossRef\]](#)
154. Papavinasam, S. Mechanisms. In *Corrosion Control in the Oil and Gas Industry*, 1st ed.; Gulf Professional Publishing: Houston, TX, USA, 2014; Chapter 5, pp. 249–300. [\[CrossRef\]](#)
155. Cord-Ruwisch, R. MIC in Hydrocarbon Transportation Systems. In *Corrosion Australasia*; Australasian Corrosion Association: Perth, WA, USA, 1995; pp. 8–12.
156. Zhang, J. RPSEA Subsea Produced Water Discharge Sensor Lab Test Results and Recommendations Final Report; Technical Report 3; Clearview Subsea LLC: Houston, TX, USA, 2016.
157. Maersk Oil. *Maersk Oil ESIA-16 Non-Technical Summary—ESIS Dan*; Technical Report; Maersk Oil: Esbjerg, Denmark, 2015.
158. Larsen, J.; Rod, M.H.; Zwolle, S. Prevention of Reservoir Souring in the Halfdan Field by Nitrate Injection. In Proceedings of the Corrosion 2004, New Orleans, LA, USA, 28 March–1 April 2004; NACE International; p. 9.
159. Thomsen, U.S.; Markfoged, R.; Meng, R.; Choong, L. Quantification of Microbiologically Influenced Corrosion in Injection Water Pipelines. In Proceedings of the Corrosion 2017, New Orleans, LA, USA, 26–30 March 2017; pp. 3676–3685.
160. Dejak, M. The Next-Generation Water Filter for the Oil and Gas Industry. *J. Pet. Technol.* **2013**, *65*, 32–35. [\[CrossRef\]](#)
161. Jepsen, K.L.; Bram, M.V.; Hansen, L.; Yang, Z.; Lauridsen, S.M.Ø. Online Backwash Optimization of Membrane Filtration for Produced Water Treatment. *Membranes* **2019**, *9*, 18. [\[CrossRef\]](#)
162. Dansk Standard. *Vandundersøgelse Suspenderet stof og gløderest: Total non Filtrable Residue and Fixed Matter in non Filtrable Residue*; Technical Report; Dansk Standard: Copenhagen, Denmark, 1985.
163. ASTM International. *Standard Specification for Woven Wire Test Sieve Cloth and Test Sieves*; Technical Report; ASTM: West Conshohocken, PA, USA, 2017. [\[CrossRef\]](#)
164. GE Healthcare. *Whatman Grade GF/D Glass Microfiber Filters, Binder Free*; GE Healthcare: Chicago, IL, USA, 2019.
165. Durdevic, P.; Raju, C.; Bram, M.; Hansen, D.; Yang, Z. Dynamic Oil-in-Water Concentration Acquisition on a Pilot-Scaled Offshore Water-Oil Separation Facility. *Sensors* **2017**, *17*, 11. [\[CrossRef\]](#) [\[PubMed\]](#)
166. Merkus, H.G. *Particle Size Measurements Fundamentals, Practice, Quality*, 1st ed.; Particle Technology Series; Springer: Dordrecht, The Netherlands, 2009; Volume 17, p. 534. [\[CrossRef\]](#)
167. Leschonski, K. Particle Characterization, Present State and possible Future Trends. *Part. Part. Syst. Charact.* **1986**, *3*, 99–103. [\[CrossRef\]](#)
168. Xu, R.; Andreina Di Guida, O. Comparison of sizing small particles using different technologies. *Powder Technol.* **2003**, *132*, 145–153. [\[CrossRef\]](#)
169. Abbireddy, C.O.R.; Clayton, C.R.I. A review of modern particle sizing methods. *Proc. Inst. Civ. Eng. Geotech. Eng.* **2009**, *162*, 193–201. [\[CrossRef\]](#)
170. Allen, T. *Powder Sampling and Particle Size Determination*, 1st ed.; Elsevier B.V.: Amsterdam, The Netherlands, 2003; p. 682. [\[CrossRef\]](#)
171. der Meeren, P.V.; Dewettinck, K.; Saveyn, H. Particle Size Analysis. In *Handbook of Food Analysis: Volume 3 Methods, Instruments and Applications*, 2nd ed.; Nollet, L.M., Ed.; Taylor & Francis: Boca Raton, FL, USA, 2004; Chapter 46, pp. 1805–1824. [\[CrossRef\]](#)
172. Leschonski, K. Representation and Evaluation of Particle Size Analysis Data. *Part. Part. Syst. Charact.* **1984**, *1*, 89–95. [\[CrossRef\]](#)
173. Berger, M. *Geometry II*, 1st ed.; Springer: Berlin/Heidelberg, Germany, 1987; p. 405. [\[CrossRef\]](#)
174. Aqra, F. Molten Alkali Halides: Straightforward Prediction of Surface Tension. *Metall. Mater. Trans. A* **2014**, *45*, 2347–2350. [\[CrossRef\]](#)
175. Ganser, G.H. A rational approach to drag prediction of spherical and nonspherical particles. *Powder Technol.* **1993**, *77*, 143–152. [\[CrossRef\]](#)
176. Hart, V.S.; Johnson, C.E.; Letterman, R.D. An Analysis of Low-Level Turbidity Measurements. *J. Am. Water Work. Assoc.* **1992**, *84*, 40–45. [\[CrossRef\]](#)
177. Bin Omar, A.; Bin MatJafri, M. Turbidimeter Design and Analysis: A Review on Optical Fiber Sensors for the Measurement of Water Turbidity. *Sensors* **2009**, *9*, 8311–8335. [\[CrossRef\]](#)
178. Broadwell, M. *A Practical Guide to Particle Counting for Drinking Water Treatment*, 1st ed.; CRC Press: Boca Raton, FL, USA, 2001; p. 240. [\[CrossRef\]](#)
179. Scardina, P.; Letterman, R.D.; Edwards, M. Particle count and on-line turbidity interference from bubble formation. *J. Am. Water Work. Assoc.* **2006**, *98*, 97–109. [\[CrossRef\]](#)
180. Fondriest Environmental Inc. *Turbidity, Total Suspended Solids and Water Clarity*; Fondriest Environmental Inc.: Fairborn, OH, USA, 2014.

181. Van Gelder, A.M.; Chowdhury, Z.K.; Lawler, D.F. Conscientious particle counting. *J. Am. Water Work. Assoc.* **1999**, *91*, 64–76. [[CrossRef](#)]
182. Shekunov, B.Y.; Chattopadhyay, P.; Tong, H.H.; Chow, A.H. Particle size analysis in pharmaceuticals: Principles, methods and applications. *Pharm. Res.* **2007**, *24*, 203–227. [[CrossRef](#)] [[PubMed](#)]
183. Karuhn, R.; Davies, R.; Kaye, B.H.; Clinch, M.J. Studies on the Coulter Counter Part I. Investigation into the Effect of Orifice Geometry and Flow Direction on the Measurement of Particle Volume. *Powder Technol.* **1975**, *11*, 157–171. [[CrossRef](#)]
184. Crowe, C.T.; Schwarzkopf, J.D.; Sommerfeld, M.; Tsuji, Y. *Multiphase Flows with Droplets and Particles*, 2nd ed.; CRC Press: Boca Raton, FL, USA, 2011; p. 509. [[CrossRef](#)]
185. Mikula, R.J. Emulsion Characterization. In *Emulsions: Fundamentals and Applications in the Petroleum Industry*, 1st ed.; Schramm, L.L., Ed.; Advances in Chemistry; American Chemical Society: Washington, DC, USA, 1992; Volume 231, Chapter 3, pp. 79–129. [[CrossRef](#)]
186. Nabipour, A.; Evans, B.J.; Sarmadivaleh, M.; Kalli, C.J. Methods for Measurement of Solid Particles in Hydrocarbon Flow Streams. In Proceedings of the SPE-Asia Pacific Oil and Gas Conference and Exhibition, Perth, Australia, 22–24 October 2012; Volume 1, pp. 702–715. [[CrossRef](#)]
187. Dansk Standard. *Particle Size Analysis—Laser Diffraction Methods*; Technical Report; DS/SO: Copenhagen, Denmark, 2009.
188. Lefebvre, F.; Petit, J.; Nassar, G.; Debreyne, P.; Delaplace, G.; Nongaillard, B. Inline high frequency ultrasonic particle sizer. *Rev. Sci. Instrum.* **2013**, *84*, 8. [[CrossRef](#)] [[PubMed](#)]
189. Adjadj, L.P.; Hipp, A.K.; Storti, G.; Morbidelli, M. Characterization of dispersions by ultrasound spectroscopy. In Proceedings of the 5th International Symposium on Ultrasonic Doppler Methods for Fluid Mechanics and Fluid Engineering (ISUD), Zürich, Switzerland, 12–14 September 2006; Volume 5, pp. 9–13.
190. McClements, D.J. Ultrasonic Measurements in Particle Size Analysis. In *Encyclopedia of Analytical Chemistry*; Meyer, R.A., Ed.; John Wiley & Sons: Chichester, UK, 2000; Chapter 6, pp. 5581–5587. [[CrossRef](#)]
191. Wrobel, B.M.; Time, R.W. Improved pulsed broadband ultrasonic spectroscopy for analysis of liquid-particle flow. *Appl. Acoust.* **2011**, *72*, 324–335. [[CrossRef](#)]
192. Zhang, J. *RPSEA Technical Gap Analysis Final Report (Phase 1 Final Report)*; Technical Report 1; Clearview Subsea LLC: Houston, TX, USA, 2015.
193. Sanderson, J. *Understanding Light Microscopy*, 1st ed.; Royal Microscopical Society; Wiley: Chichester, UK, 2019; Chapter 30, p. 815. [[CrossRef](#)]
194. Shand, R.M. User manuals as project management tools. II. Practical applications. *IEEE Trans. Prof. Commun.* **1994**, *37*, 123–142. [[CrossRef](#)]
195. Canty, T.M.; O'Donoghue, A.; Relihan, E. Inline Oil in Water Particle Analysis and Concentration Monitoring for Process Control and Optimisation in Produced Water Plants. In Proceedings of the TUV NEL's 7th Produced Water Workshop, Aberdeen, UK, 29–30 April 2009; TUV NEL; p. 8.
196. Christensen, K.M. *Installation and Testing of a Jorin Visual Process Analyzer Analyzer*; Technical Report; Idaho National Laboratory, Fuel Cycle Research and Development: Idaho Falls, ID, USA, 2010.
197. Pontius, K. *Monitoring of Bioprocesses Opportunities and Challenges*; Technical University of Denmark: Lyngby, Denmark, 2019.
198. Højris, B.; Christensen, S.C.B.; Albrechtsen, H.J.; Smith, C.; Dahlgvist, M. A novel, optical, on-line bacteria sensor for monitoring drinking water quality. *Sci. Rep.* **2016**, *6*, 1–10. [[CrossRef](#)] [[PubMed](#)]
199. Panckow, R.P.; Comandè, G.; Maaß, S.; Kraume, M. Determination of Particle Size Distributions in Multiphase Systems Containing Nonspherical Fluid Particles. *Chem. Eng. Technol.* **2015**, *38*, 2011–2016. [[CrossRef](#)]